Algal Research 81 (2024) 103555

Contents lists available at ScienceDirect

Algal Research

journal homepage: www.elsevier.com/locate/algal

Short-term effects of light quality, nutrient concentrations and emersion on the photosynthesis and accumulation of bioactive compounds in *Pyropia leucosticta* (Rhodophyta)

Julia Vega [a,*], Bruna R. Moreira [b], Antonio Avilés [a], José Bonomi-Barufi [b], Félix L. Figueroa [a]

[a] Universidad de Málaga, Instituto Andaluz de Biotecnología y Desarrollo Azul (IBYDA), Centro Experimental Grice Hutchinson, Lomas de San Julián, 2, 29004 Málaga, Spain
[b] Departamento de Botânica, Centro de Ciências Biológicas, Universidade Federal de Santa Catarina, 88040-970 Florianópolis, SC, Brazil

ARTICLE INFO

Keywords:
Biliproteins
Blue and violet light
Emersion
Integrated electron transport rate
Mycosporine-like amino acids
Ultraviolet A radiation

ABSTRACT

Intertidal macroalgae have developed adaptation and acclimation strategies protecting against stressful environments. The red algae, *Porphyra* sensu lato are well known for their use as human food, but they also present potential applications in cosmeceutics. In order to enhance the content of interested bioactive compounds, this study evaluated the effects of three different stress factors, through two bi-factorial experiments, the combination of PAR and PAR supplemented by UV-A, Violet and Blue radiation ($PAR_{UVAViBl+}$) with three nutrient concentrations or emersion/immersion conditions. Interactive effects of $PAR_{UVAViBl+}$ and nutrient concentrations on the daily integrated electron transport rate (ETR_{int}) was observed. This suggests a photoprotective effect of nitrate against the possible damage by UV-A radiation. The emersion produced a decreased in the *in situ* ETR, followed by a recovery during re-hydration. The energy dissipation rate (EDR), firstly described in this work, increased under nutrient limitation and under $PAR_{UVAViBl+}$ radiation, as a photoprotection mechanism. At morphological level, the surface/volume (S/V) ratio of the cells increased under nutrient limitation favoring the nitrogen assimilation, although it could be a risk of photodamage under UV-A radiation. Biliproteins and mycosporine-like amino acids (MAAs) increased under high nutrient availability as it was expected due to both are N-compounds. Polyphenols were higher under $PAR_{UVAViBl+}$ at day 2, indicating a photoprotective mechanism whereas this effect disappeared at day 7 of culture. Emersion seems to induce MAAs accumulation under $PAR_{UVAViBl+}$ radiation. Antioxidant capacity determined by ABTS assay was positively correlated to antioxidant substances as biliproteins, polyphenols and MAAs. The application of short-term stress conditions (2–7 days) during culture, can be a strategy to increase the content of interesting compounds due to both UV screen properties and antioxidant capacity.

1. Introduction

Intertidal macroalgae have developed different adaptation and acclimation strategies to protect themselves against a harsh and highly variable environment (e.g. periods of desiccation, high solar radiation, hydrodynamics or changing temperature and salinity), such as strong antioxidant defense systems (e.g. catalase or superoxide dismutase enzymes), the synthesis of secondary metabolites with antioxidant, photoprotective or anti-herbivory properties (e.g. phenolic compounds, carotenoids or mycosporine-like amino acids -MAAs-), photorepair mechanisms (e.g. photolyases) and energy dissipation mechanisms (i.e. non photochemical quenching) [1,2]. Beside these, the synthesis of primary metabolites, that are mainly implicated in physiological and structural functions (e.g. amino acids, proteins, lipids or polysaccharides), also play an important role in the protection against environmental factors [3–6].

Macroalgae have acquired a great biotechnological interest in the last years, due to the wide diversity of bioactive compounds with several potential applications. Among the bioactive compounds found in macroalgae, three of them are highlighted in this study: biliproteins, phenolic compounds and MAAs. Biliproteins as accessory pigments are involved in the light absorption for photosynthesis in some algae species (Rhodophyta, Cyanobacteria and Cryptophyta). These compounds have been used as fluorescent probes in immunofluorescence assay, food

* Corresponding author.
E-mail address: juliavega@uma.es (J. Vega).

https://doi.org/10.1016/j.algal.2024.103555
Received 2 August 2023; Received in revised form 20 February 2024; Accepted 25 May 2024
Available online 4 June 2024

additives or natural colorants in ice-creams, candies, or soft drinks. In addition, different therapeutic properties have been described to these molecules, such as antioxidant, anti-cancer, neuroprotective, anti-inflammatory, antiviral or hepatoprotective [7,8]. Phenolic compounds are secondary metabolites, that can be found in plants and algae. Among algae, brown algae normally present the highest content [9–12]. These compounds act as protective agents that are synthetized in response to stress conditions like herbivory or UV radiation. Several bioactivities with potential pharmaceutical properties have been described in these compounds: antioxidant, anti-inflammatory, antimicrobial, antiviral, antidiabetic, anticancer or neuroprotective [13,14]. MAAs are secondary metabolites, mainly found in red algae and cyanobacteria and they are involved in photoprotection. These molecules have been considered potential compounds to be used as natural UV filters in sunscreens, due to their capacity to absorb the UV radiation, their no-toxicity and biodegradable properties. In addition, different beneficial properties for the skin have been described in these molecules, such as antioxidant, anti-inflammatory, wound-healing or anti-aging [15–17].

The physiology and biochemical composition of algae can be influenced by the environmental factors such as light quality, nutrients availability or desiccation. Modify or control these factors during algae culture can influence the growth or induce the accumulation of specific compounds. Light quality can affect photosynthesis through both photosynthetic process [18,19] and the regulation of some physiological responses by the action of non-photosynthetic photoreceptors in photomorphogenic process (e.g. cryptochromes or phytochromes) [20,21]. Thus, different authors have analyzed the effect of different light qualities in algal culture. Some of them cultivated algae under broad band light colors, using white light lamps with different filters [18,22–24], and other researchers studied the photomorphogenic responses of different light qualities, by adding a small light supplementation by using LEDs (5–20 %) of UV-A, blue, green, or red radiation to a saturating photosynthetic irradiance produced by amber light [19,25,26]. Most reports observed that UV-A radiation and blue light increased the accumulation of certain compounds such as MAAs or biliproteins in different red alga species, or that supplementation of UV-A radiation (as green or red light) can increase growth, but reduce the photosynthetic rate. In this work, the combination of UV-A, violet and blue radiation is studied (320-450 nm), since all of them could be potentially detected by the same photoreceptor, the cryptochrome, and in addition possible photodamage by UVA radiation can be also detected [27].

In relation to the nutrient availability, high nitrogen conditions increased the photosynthetic capacity, growth, as well as the accumulation of N-compounds (e.g. proteins, phycobiliproteins or MAAs) [28–30]. In addition, the nitrogen enrichment has shown a protective role against different environmental stressed conditions, compensating or reducing their negative effects. Gao et al. [31] observed that with high nitrogen concentration, *Pyropia yezoensis* was able to maintain the growth and net photosynthesis under ocean acidification conditions (high carbon) [31]. Barufi et al. [32] also observed that nitrate can reduce the negative effects of UV radiation on photosynthesis in *Gracilaria tenuistipitata* due to the accumulation of MAAs. The culture of red algae under Integrated multitrophic aquaculture (IMTA) systems (high nitrogen supply through fishpond effluents) have been analyzed by some researchers, both inland or open water systems [33–37] obtaining promising results with high nitrogen uptake rates and biomass productivity, and the accumulation of certain compounds with commercial application such as biliproteins or MAAs.

As mentioned before, intertidal algae face periods of desiccation, although not all of them tolerate it in the same way. According to Contreras-Porcia et al. and Lalegerie et al. [1,38] "desiccation tolerance is known as the ability to withstand a significant water loss and a fast recovery during re-hydration, and not the ability to retain water". There are tolerant species, those that live in the upper intertidal zone, e.g. *Porphyra* spp. can lose >90 % of the internal water content, follow by a fast recovery after de-hydration [39,40]. By contrast, those species living in the lower intertidal zone are more sensitive to desiccation, e.g. *Gelidium rex* does not recover after re-hydration [41]. Desiccation can provoke different morphological, biochemical or physiological responses in macroalgae. For example, Contreras-Porcia et al. [39] observed morphological changes in *P. columbina* during low tides desiccation, showing that dehydrated fronds become dark purple, tightly folded, stiff and brittle, as a strategy to prevent the rupture of the plasma membrane. Li et al. [42,43] observed an increase of carotenoids and biliproteins in *Pyropia yezoensis* submitted to emersion conditions. This is considered as a positive role in the quality of the biomass due to the algal tissue colour.

Bladed Bangiales *(Porphyra* sensu lato*)* are common species globally distributed in intertidal zones, although they are more abundant in cold temperate waters. These species present one cell layer and are characterized by their elastic thalli, high resistance to desiccation and a seasonal cycle (i.e. a macroscopic phase, folious blades, can be observed during winter, whereas the summer (long photoperiod and warm temperatures) promotes the sporulation and the microscopic filamentous conchocelis phase). *Pyropia leucosticta* is commonly found in the intertidal Mediterranean coast, sharing habitats with other macroalgae as *Rissoella verrucullosa* (endemic to the Mediterranean Sea), *Nemalion helminthoides or Ulva* sp. [44,45]. *Porphyra* sensu lato are commercially known as nori or laver and are among the most cultured macroalgae in the world (mainly concentrated in Asian countries), with an economic value that is growing over the years [46,47]. During its culture, it is normally submitted to periodical desiccation to avoid the presence of epiphytes [48]. Besides their known utilization as human food (e.g. nori blades for sushi), *Porphyra* sensu lato could be source of bioactive compounds with relevant industrial applications, such as the mentioned molecules, e.g. MAAs could be used is cosmeceutic products due to their photoprotective properties [17,49].[NO_PRINTED_FORM].

Considering that algal metabolism must be fitted to so harsh environmental variable conditions, and that *P. leucosticta* is a relevant species for biotechnological applications, our study aimed to evaluate the effects of three physiological regulating parameters (UVA-Violet-Blue radiation, nutrients concentration and emersion) in the photosynthesis, morphology and accumulation of bioactive compounds, through two bi-factorial experiments in laboratorial conditions, combining UVA-Violet-Blue radiation and nutrient concentrations and emersion/immersion conditions.

2. Material and methods

2.1. Algae biomass

Pyropia leucosticta (Bangiales, Rhodophyta) thalli were collected in January 2021 from Lagos (Malaga, Southern Spain; 36°44′N; 4°01′W). Algae were transported to the laboratory in a portable fridge at 4 °C and cleaned to remove sediments and epiphytes. Algae were maintained in polyvinyl methacrylate cylinders (1 L seawater) during two weeks before the start of the experiments. Algae were maintained at an algal density of 10 g fresh biomass (FB) L^{-1} at 20 °C, salinity 36, irradiance of photosynthetic active radiation (PAR, λ = 400–700 nm) of 150 μmol photons m^{-2} s^{-1} (White LED light, 5000 K, 54 W, NU-8416, Nuovo) with a photoperiod of 12:12 h (light:dark) and under low nutrient concentration (50 μM $NaNO_3$ and 2.7 μM of $C_3H_7Na_2O_6P$ added each week), before the starting of the experiments.

2.2. Experimental design

In this study, two different bi-factorial experiments were performed on *P. leucosticta*. The first one considered the effects of two light qualities: PAR and PAR supplemented by UV-A, Violet and Blue radiation ($PAR_{UVAViBl+}$), and nutrient availability (three different concentrations);

and the second one, the effects of the same two light qualities and emersion/immersion conditions. All treatments were performed in triplicate.

The radiation treatment was the same in both experiments: PAR (λ = 400–700 nm), provided by a white LED light (5000 K, 54 W, NU-8416, Nuovo), and PAR supplemented with UV-A (λ = 320–400 nm), violet (λ = 400–450 nm) and blue light (λ = 450–500 nm). The supplementation was obtained combining a fluorescent UV-A lamp (UVA340, Q-Lab Corporation, Canada) with a Lee-130 filter [50] to cut-off the UV-B radiation, and an UVA-Violet-Blue LED lamp (Aralab, Portugal), that present peaks at 370, 406 and 446 nm (Fig. 1A; Fig. SM.1). This combination of UV-A, Violet and Blue radiation was applied considering the already knowledge on the photocontrol by non photosynthetic UVA/Blue photoreceptor (Cryptochromes) in the synthesis of different bioactive compounds in macroalgae, including *Porphyra* spp. [20,22,51–53].

To simulate a daily cycle of natural radiation, PAR irradiance increased from 150 to 300 μmol photons m^{-2} s^{-1} during the central period of the day (13–17 pm). The supplemented radiation was also provided during this period at the irradiances of 8 W m^{-2} of UV-A and 70 μmol photons m^{-2} s^{-1} of violet-blue light, corresponding to a supplementation of 15 % of UV-A and 30 % of violet-blue radiation (Fig. 1B). The white light used for the PAR treatment already have a peak in blue (446 nm), and the $PAR_{UVAViBl+}$ treatment was supplemented with more blue (446 nm) and other two peaks of 365 nm (UV-A) and 404 nm (violet). The irradiance of PAR was measured using a radiometer (LI-1000 Data Logger, LI-COR Biosciences, USA) with a flat sensor (LI-190R quantum sensor, LI-COR Biosciences, USA). The spectrum of the different lamps and the irradiance of the UV radiation was measured by using a spectroradiometer (SMS 500, Sphere Optics, Germany). The daily integrated irradiances received by algae in each treatment are shown in Table 1. The supplemented radiation (UV-A and Violet-Blue) represents an increase in the daily dose of 4 % for UV-A radiation, and 15 % for Violet-Blue radiation. The calculated effective radiation doses against five different action spectra: photosynthesis [54], chloroplast photoinhibition [55], DNA damage [56], general damage in plants [57] and lipid peroxidation [58] (Fig. SM.2) are shown in Table 2.

In the first experiment, three different nutrient concentrations were tested: 500 + 27.7, 250 + 13.8 and 50 + 2.7 μM of $NaNO_3$ and

Table 1
Daily radiation doses received (kJ m^{-2} day^{-1}) in each light treatment (P and P_{UVAVB+}) during the experimental period. The doses were also calculated for different fractions of the full spectra received in each treatment.

	PAR	$PAR_{UVAViBl+}$
UV-B (280–320)	0.22	1.00
UV-A (320–400)	0.86	54.71
Violet + Blue (400–500)	359.88	577.13
$PAR_{without\ Vi+Bl}$ (500–700)	1031.40	1033.22
PAR (400–700)	1391.28	1610.35
TOTAL	1392.36	1666.10

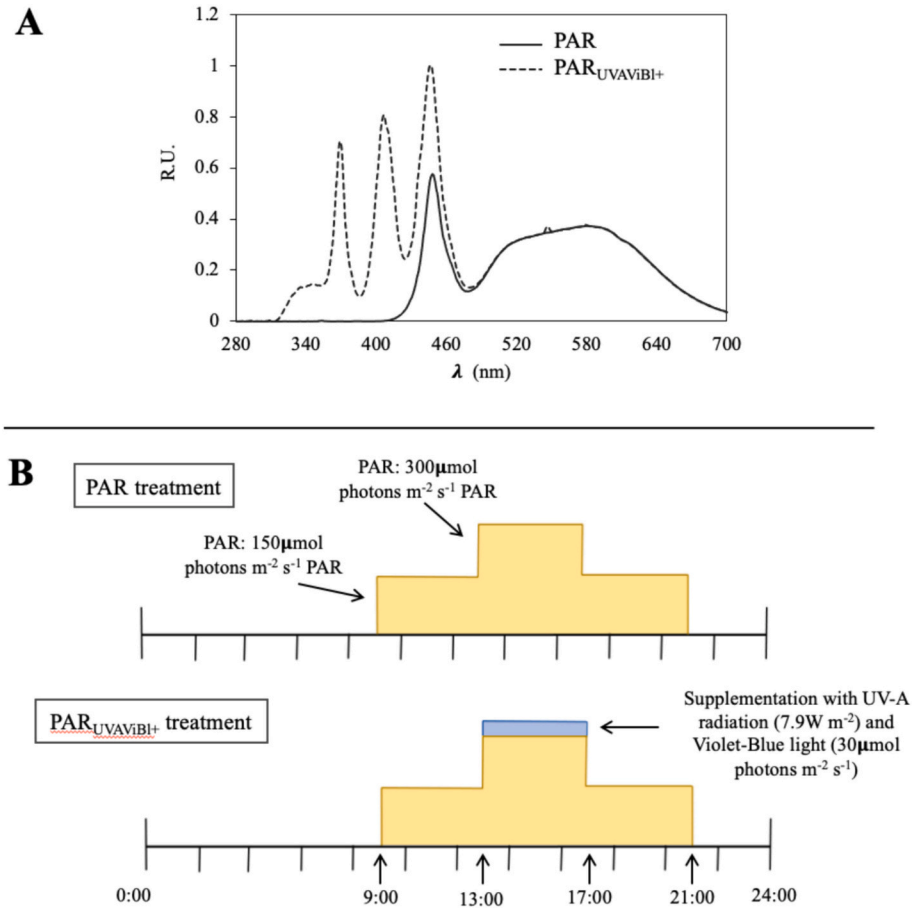

Fig. 1. Experimental design of the radiation treatment used in both experiments with *Pyropia leucosticta* evaluating: (1) the effect of supplemented light treatment with UV-A, violet and blue radiation ($PAR_{UVAViBl+}$) and nutrient concentrations (500, 250 and 50 μM $NaNO_3$), and (2) the effect of $PAR_{UVAViBl+}$ and emersion/immersion condition. A) Spectra of the two radiation treatments used in the experiments. B) Design of the radiation treatments. PAR was provided from 9:00 to 21:00. During central hours of the day (13:00 to 17:00), PAR irradiance increased, and samples also received supplementation of UVA-Violet-Blue radiation. (For interpretation of the references to color in this figure legend, the reader is referred to the web version of this article.)

Table 2
Daily effective radiation doses received (kJ m^{-2} day^{-1}) related to different biological responses (photosynthesis, DNA damage, chloroplast photoinhibition, general damage in plants and lipid peroxidation) driven by UVR and PAR, in each radiation treatment (P = PAR; $P_{UVAViBl+}$ = PAR $_{UVAViBl+}$) during the experimental periods. The doses were also calculated for different fractions of the full spectra received in each treatment.

	Photosynthesis		DNA damage		Chloroplast photoinhibition		General damage in plants		Lipid peroxidation	
	P	$P_{UVAViBl+}$	P	$P_{UVAViBl+}$	P	$P_{UVAViBl+}$	P	$P_{UVAViBl+}$	P	$P_{UVAViBl+}$
UV-B (280–319)	0.00	0.00	0.03	0.08	0.13	0.50	0.08	0.23	0.10	0.31
UV-A (320–399)	0.00	0.00	0.00	0.00	0.11	7.11	0.00	0.27	0.03	1.69
Violet-Blue (400–499)	64.47	95.30	0.00	0.00	0.00	0.32	0.00	0.02	0.00	0.05
$PAR_{without\ Vi+Bl}$ (500–700)	639.61	641.02	0.00	0.00	0.00	0.00	0.00	0.00	0.00	0.00
PAR (400–700)	704.08	720.53	0.00	0.00	0.00	0.32	0.00	0.02	0.00	0.05
TOTAL	768.55	815.83	0.03	0.08	0.24	8.25	0.08	0.54	0.12	2.11

$C_3H_7Na_2O_6P$, respectively. Provasoli medium [59,60] was added in all cylinders and only $NaNO_3$ and $C_3H_7Na_2O_6P$ were modified for the different treatments. After five days of the experimental period, half of nitrate and phosphate compared to initial values were added.

To achieve algal emersion, a net was placed at the bottom of the cylinder, and during the central hours of the day (13-17 pm), the net was raised so that algae were out of the water during this period. In those cylinders with no emersion, a net was also placed at the bottom of the cylinders and it was also raised, although algae were maintained covered by the water in the upper part of the cylinder.

During the experiments, algae were maintained at a concentration of 5 g L^{-1}, at 20 °C and salinity 36. Both experiments were conducted for seven days. In the second experiment enriched seawater (Provasoli medium) was also added to all cylinders with the normal nitrate and phosphate concentration (500 μM of $NaNO_3$ and 27.7 μM $C_3H_7Na_2O_6P$). In the fifth day of the experiment, 50 μM of nitrate and 2.7 μM phosphate were also added.

Algae growth rate, as percentage of daily growh rate (% DGR), was calculated as Lignell & Pedersen [61].

Different parameters were assessed during both experimental periods. Nitrogen uptake rate (NUR) was analyzed from seawater samples. Photosynthesis was followed by *in vivo* chlorophyll *a* fluorescence of photosystem II (PSII). Biochemical composition and antioxidant capacity were determined by using different spectrophotometric and chromatographic procedures in biomass from day 2 (500 mg of fresh biomass were collected) and from day 7 (end of the experimental period). Microscopic analysis was only performed in biomass collected at the end of the experiment. The biomass was collected after several hours of the stressed condition (i.e. $PAR_{UVAViBl+}$ or emersion condition).

2.3. Nitrate uptake rate (NUR)

For nutrients analysis, 10 mL of water were collected from the culture cylinders at day 0, 2, 5 and 7 for the first experiment, and at day 0, 3, 5 and 7 for the second experiment. At day 5, water was sampled before and after the addition of new nutrient input. Water samples were filtered through 0.45 μM and frozen at −20 °C until analysis. Total nitrate contents were analyzed by segmented flow analyzer (SFA) using a Seal Analytical autoanalyzer QuAAtro following the methods described by Grasshoff et al. [62]. The detection limits of the inorganic nutrients were 0.05 μM. The nitrate uptake rates (NUR) were calculated according to the following formula and expressed as μmol $NaNO_3$ L^{-1} day^{-1}.

$$NUR = (C_1 - C_2/t$$

where C_1 and C_2 are the initial and final concentrations expressed as μmol $NaNO_3$, and t is the time expressed as days.

2.4. Photosynthetic activity by using in vivo chlorophyll a fluorescence

The photosynthetic activity of *P. leucosticta* was estimated through the *in vivo* chlorophyll *a* fluorescence associated to photosystem II (PSII), using a Mini-PAM-II (Walz GmbH, Germany). Two different approaches were followed:

2.4.1. In situ measurements

In vivo chlorophyll *a* fluorescence was measured *in situ*, i.e. under the growth conditions in the culture chambers, during different days and periods of the day. In the first experiment (light quality and nutrients), it was monitored during days 0, 2, 5 and 7, and at 8:30, 10:00, 14:00 and 18:00. In the second experiment (light quality and emersion) it was determined during days 0, 3, 6 and 7 at 8:30, 10:00, 14:00, 16:00 and 18:00. For that, saturating pulses (> 3000 μmol photons m^{-2} s^{-1}) were applied to algal thalli (three replicates per cylinder) during darkness of the daily photoperiod (8:30 am) and at different times during the light cycle, in order to quantify the basal (F_o), steady-state (F_t) and the maximal fluorescence (F_m measured in samples at darkness or F_m' in light-acclimated samples). Optimal quantum yield (F_v/F_m) and the effective quantum yield (Y(II)) were calculate as follows:

$$F_v/F_m = (F_m - F_o)/F_m$$

$$Y(II) = (F_m' - F_t)/F_m'$$

Electron transport rate (ETR; μmol electrons m^{-2} s^{-1}) values were calculated using the following formula:

$$ETR = Y(II)\ x\ E_{PAR}\ x\ A\ x\ F_{II}$$

where E_{PAR} is the irradiance in the PAR region of the spectra (λ = 400–700 nm) and expressed as μmol photons m^{-2} s^{-1}, A is the absorptance that was calculated as A = 1-(E_t/E_0) (E_t is the irradiance that pass through the thallus and E_0 is the emitted irradiance), and F_{II} is the fraction of chlorophyll *a* associated to PSII, in red algae is 0.15 [63–65]. The ETR values obtained for each day were integrated using the trapezoidal rule, allowing the calculation of $_{int}$ETR (integrated ETR).

2.4.2. Rapid light curves (RLC) and yield losses

Before the starting of the rapid light curves (RLCs), algae were incubated in darkness for 15 min, in order to oxidize the reaction centers. During RLCs, algae were incubated during 30 s at increasing irradiances (from 0 to 1500 μmol photons m^{-2} s^{-1}) of the actinic red light of the Mini-PAM-II. After incubation at each intensity, a saturating pulse was performed. Different parameters were calculated for each intensity of the RLCs: F_v/F_m, Y(II), ETR, two different yield losses: Y(NPQ) calculated as (F_t/F_m')-(F_t/F_m) and Y(NO) calculated as F_t/F_m, and non-photochemical quenching (NPQ) calculated as Y(NPQ)/Y(NO). Similarly to Figueroa et al. [2], it was calculated the amount of absorbed energy used in photochemistry (ETR) and amount of absorbed energy that is dissipated (yield losses), named as energy dissipation rate (EDR) and calculated as ETR, but replacing Y(II) values for the sum of both yield losses (Y(NPQ) + Y(NO)), and it was expressed as μmol photons m^{-2} s^{-1}:

$$EDR = (Y(NO) + Y(NPQ))\ x\ E_{PAR}\ x\ A\ x\ F_{II}$$

The obtained ETR vs. irradiance, curves were fitted according to Eilers and Peters [66]. The following RLC descriptive parameters were

obtained: ETR_{max}, photosynthetic efficiency (α_{ETR}) and saturated irradiance (Ek_{ETR}).

Previously to the experiments, a RLC and an in situ light curve ($LC_{in\ situ}$) were performed, in order to determine the appropriate PAR irradiances during experiments (Fig. SM.3). For the $LC_{in\ situ}$, algae were incubated for one minute to increasing irradiances of the white LED light (from 0 to 700 μmol photons m^{-2} s^{-1}). The Ek values obtained were 130 and 175 μmol photons m^{-2} s^{-1} from RLC and LC *in situ*, respectively. So, an irradiance of 150 μmol photons m^{-2} s^{-1} was selected.

2.5. Microscopic analyses

Microscopic images were made on algal thalli immerse in 20 % glycerine, using the Olympus VS120 (Tokio, Japan) virtual microscopy slide scanning. The processing of the obtained images was done with the software ImageJ. The following parameters were calculated from the surface view: (a) number of cells, (b) percentage occupied by the protoplasm, and (c) average size of the protoplasm.

2.6. Biochemical analysis

All biochemical analyses were performed from the fresh weight (FW), except total carbon, nitrogen and sulphur content that need dry weight (DW). The ratio FW/DW was calculated as 5.5 and all results were expressed as mg g^{-1} DW. Biochemical analyses were performed at day 0, 2 and 7 for the first experiment, and at day 0, 3 and 7 for the second experiment (except total carbon, nitrogen and sulphur content in the second experiment, that was only determined at day 7).

2.6.1. Total internal carbon, nitrogen and sulphur

Total carbon, nitrogen and sulphur content were determined from dry biomass using an elemental analyzer (CNHS LECO-932, Michigan, USA) in the Research Support Central Services (SCAI, University of Malaga).

2.6.2. Photosynthetic pigments

For phycobiliproteins determination, 50 mg of FW were homogenized in 1.5 mL of phosphate buffer (pH 6.5, 0.1 M) using pistil, mortar, and sand as abrasive. After overnight incubation at 4 °C, samples were centrifuged (Heraeus Labofuge 400R, Thermo Scientific, Waltham, MA, USA) and measured by using a spectrophotometer (UV-2600, Shimadzu, Duisburg, Germany) at the following wavelengths: 455, 564, 592, 618, 645 and 730 nm. Quantification was made using the chromatic formulas described by Beer & Eschel [67] for phycoerythrin (PE) and phycocyanin (PC).

In the case of chlorophyll *a* determination, 50 mg of FW were homogenate in 1.5 mL of 90 % acetone saturated with magnesium carbonate using pistil, mortar, and sand as abrasive. After incubation (4 °C overnight) and centrifugation, extracts were spectrophotometrically measured at the following wavelengths: 664, 691 and 750 nm, and total of chlorophyll *a* was quantified according to Ritchie et al. [68].

2.6.3. Phenolic compounds

Phenolic compounds were measured using the Folin-Ciocalteau method according to Singleton and Rossi [69] with some modifications. Fifty mg of FW were extracted in 1.5 mL of methanol 80 % using pistil, mortar, and sand as abrasive, and remained overnight at 4 °C. After centrifugation, 100 μL of the extracts was mixed with 700 μL of $_dH_2O$ and 50 μL of Folin-Ciocalteau reagent (Sigma-Aldrich, San Luis, MO, USA). The mixture was vortexed and 150 μL of $NaCO_3$ 20 % was added to the mixture and vortexed again. Samples were incubated during 2 h at 4 °C and measured by a spectrophotometer described above at 760 nm. Phloroglucinol (Sigma-Aldrich, San Luis, MO, USA) was used as standard.

2.6.4. Mycosporine like amino-acids (MAAs)

MAAs was determined using a uHPLC according to Korbe-Peinado et al. [28] with some modifications of Chavez-Peña et al. [70], i.e. resuspension of the samples in water instead of methanol. Fifty mg of FW were incubated in 1.5 mL of 20 % methanol in water during 2 h at 45 °C in a water bath. After that, samples were centrifuged and 700 μL of the supernatant were dried under vacuum (Speed-Vac SPD210, Thermo Scientific, Waltham, MA, USA). The dried samples were re-suspended in 700 μL of ultrapure H_2O, filtered through a 0.2 μm filter and injected in the uHPLC (1260 Agilent InfinityLab Series, Santa Clara, CA, USA). MAAs were detected using a Luna C8 column (Phenomenex, Aschaffenburg, Germany), applying an isocratic flow of 0.5 mL min^{-1} and a mobile phase of 1.5 % methanol and 0.15 % acetic acid in ultrapure H_2O. The detection was made using a photodiode array detector at 330 nm. Isolated MAAs through HPCCC [71] were used as standards. Quantification was performed using the molar extinction coefficients (ε) of the different MAAs [72]. Results were expressed as mg g^{-1} DW.

2.7. Antioxidant capacity

Two different methods based on the free radical scavenging effect were used to determine the antioxidant capacity.

The ABTS assay was performed according to Re et al. [73] with some modifications. The ABTS radical cations ($ABTS^{+\cdot}$) were generated via a reaction of 7 mM ABTS (2,2′-azino-bis(3- ethylbenzothiazoline-6-sulfonic acid; Sigma-Aldrich, San Luis, MO, USA) and 2.45 mM $K_2S_2O_8$ in phosphate buffer (0.1 M, pH:7). This reaction was stored for 12–16 h at room temperature to ensure the complete formation of the radical. $ABTS^{+\cdot}$ solution was diluted with phosphate buffer until the absorbance at 727 nm was around 0.75 ± 0.05. The same extracts prepared for phycobiliproteins quantification were used in this assay. For the reaction, 50 μL of the extracts were mixed with 950 μL of the diluted $ABTS^{+\cdot}$. The mixture was incubated for 8 min at room temperature and darkness, and absorbances were measured at 727 nm.

The DPPH assay was made according to Brand-Williams et al. [74] with some modifications. The same extracts prepared for phenols quantification were used in this assay. For the reaction, 200 μL of the extracts were mixed with 1 mL of the DPPH• (2,2-diphenyl-1-picrylhydrazyl; Sigma-Aldrich, San Luis, MO, USA) solution (0.06 mM of DPPH in methanol 80 %). After 30 min of incubation at room temperature and darkness, absorbances were measured at 517 nm.

For both methods, a standard solution of Trolox (6-hydroxy-2,5,7,8-tetramethylchroman-2-carboxylic acid; Sigma-Aldrich, San Luis, MO, USA) was used as reference and the results were expressed as μmol TE (Trolox equivalent) g^{-1} DW.

2.8. Statistics

The software STATISTICA (V7) were used for the statistical analysis. Initially, data were checked for normality (Kolmogorov-Smirnov test) and homogeneity of variances (Cochran test). Then, two-way analyses of variance (ANOVA, $p < 0.05$) were used for the comparison of the treatments in the different analyzed variables. In the case of the first experiment, the factors were radiation (two levels: PAR and PAR + UVAVB) and nutrients availability (three levels: 500, 250 and 50 μM NO_3). For the second experiment, the factors were also radiation (same two levels) and emersion/immersion conditions (two levels: emersion (EMER) and immersion (IMMER)). These analyses were conducted separately for each time period. Newman-Keuls post-hoc test was used to identified homogenous groups after significant interaction in the ANOVA. Student-*t*-test were used to compared obtained values with initial ones ($p < 0.05$). Pearson's correlation analysis was used to observed positive or negative correlations between dependent variables ($p < 0.05$ or 0.01).

3. Results

3.1. Growth and nutrient uptake rates

An increment of algal biomass during the experimental period was not observed, i.e. the algal weight remained constant. However, during the acclimation period (two weeks), algae grew 1.2 % day^{-1}. The nutrient uptake rates (NUR) during both experimental periods are presented in the Table SM.1. In the first experiment (light quality and nutrients), significant differences in the NUR were only observed among nutrients concentrations (no effect of the light quality was obtained) in both analyzed periods (Table SM.3). The highest NUR were observed in the treatment with the highest nutrient availability. During the first period of the experiment (0–2 days), the highest NUR were 245.4 μmol $NaNO_3$ L^{-1} day^{-1}, whereas in the last period (5–7 days) with a lower nutrients addition, the highest NUR were 111.4 μmol $NaNO_3$ L^{-1} day^{-1}. During the second experiment (light quality and emersion/immersion), significant interaction between treatments were observed in the first periods of the culture (0–3 days), whereas in the last period (5–7 days) no significant differences were obtained (Table SM.4). Significant differences were only observed in algae culture with $PAR_{UVAViBl+}$ under immersion and emersion conditions (146.7 and 101.4 μmol $NaNO_3$ L^{-1} day^{-1}, respectively).

3.2. Photosynthetic parameters (in situ and ex situ)

In situ electron transport rate (ETR) during the experimental period in both experiments is shown in fig. SM.4. In all cases, there is an increment of in situ ETR in the middle of the day, followed by a decrease at the afternoon. In order to compare the different treatments, the integrated daily ETR (ETR_{int}) of the different treatments were calculated for each day (Fig. 2). In case of the first experiment, no significant interaction between the studied factors were observed during the first day of the experiment, whereas significant effects in the treatments of each factor separately was observed (Table SM.3). In this day, algae under $PAR_{UVAViBl+}$ treatment presented a lower ETR_{int} (0.27 mol e^- m^{-2}), than algae under PAR treatment (0.28 mol e^- m^{-2}). Algae submitted to the lowest nutrient concentration (50 μM) showed the lowest ETR_{int} (0.26 mol e^- m^{-2}), in comparison with the other nutrient concentrations. In the rest of the experiment (day 2, 6 and 7) significant interaction between variables was obtained (Table SM.3). At day 7, the lowest ETR_{int} was obtained in the treatments with low nutrients (50 μM; 0.19 mol e^- m^{-2}), followed by the $PAR_{UVAViBl+}$ and 250 μM nitrate treatment (0.24 mol e^- m^{-2}), and for the rest of the treatments (PAR 500, PAR 250 and $PAR_{UVAViBl+}$ 500) without significant differences among them (0.31 mol e^- m^{-2}). In relation with the second experiment, significant differences between factors separately (no significant interaction) were observed in the first day of the experiment (Table SM.4). Higher ETR_{int} values were observed in algae under $PAR_{UVAViBl+}$ radiation (0.35 mol e^- m^{-2}) than in algae under only PAR (0.32 mol e^- m^{-2}). Higher values were also observed in those algae with emersion (EMER: 0.35 mol e^- m^{-2}) than in algae under no emersion (IMMER; 0.32 mol e^- m^{-2}). In the third day of the experiment, significant interaction among factors was obtained (Table SM.4), differences were only observed between the $PAR_{UVAViBl+}$ and IMMER (0.36 mol e^- m^{-2}) treatment and the others (0.32 mol e^- m^{-2}). At the end of the experiment (day 5 and 7), the interaction between factors disappeared (Table SM.4), and significant differences were only observed between immersed or emersed conditions. Algae under immersed condition showed a highest ETR_{int} (EMER: 0.29 mol e^- m^{-2}; IMMER: 0.33 mol e^- m^{-2}).

In Table 3, different values obtained from the RLCs at end of the experimental periods are shown. In case of the first experiment, F_v/F_m values showed interaction between factors (Table SM.3). The lowest value was obtained in the treatment $PAR_{UVAViBl+}$ 50 (0.56) and the highest value was observed in the P 500 (0.7). Significant difference with the initial value (0.65) were only observed in the $PAR_{UVAViBl+}$ 50 treatment (0.56). The ETR_{max} values only showed significant differences among nutrients concentrations (Table SM.3). The ETR_{max} varied from 2.15 μmol e^- m^{-2} s^{-1} in the treatments with low nutrients (50), to 2.97 μmol e^- m^{-2} s^{-1} in the treatments with high nitrogen (500). Significant differences with the initial value (3.83 μmol e^- m^{-2} s^{-1}) were observed in the treatments PAR 50, $PAR_{UVAViBl+}$ 250 and $PAR_{UVAViBl+}$ 50 (2.30, 2.17 and 2.01 μmol e^- m^{-2} s^{-1}, respectively). α_{ETR} and Ek_{ETR} values did not shown significant differences among the treatments (Table SM.3) or with the initial value. The average values of α_{ETR} and Ek_{ETR} were 0.03 and 110.84 μmol photons m^{-2} s^{-1}, respectively. In the second experiment, no significant differences were observed in any of the variables (Table SM.4). Significant differences with the initial values were only

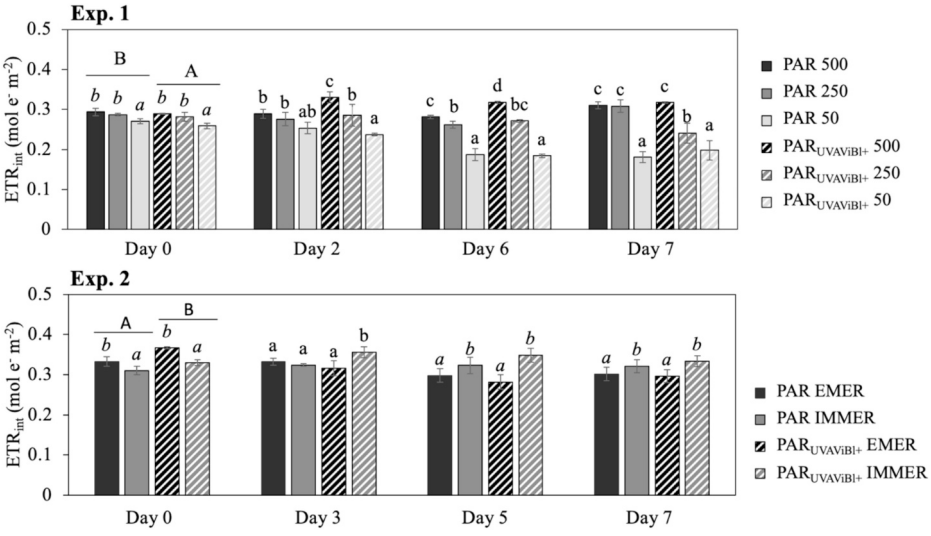

Fig. 2. Integrated electron transport rate (ETR_{int}) calculated with the in situ measurements show in fig. SM.4 in both experiments with *Pyropia leucosticta*: Exp. 1) light quality and nutrients (500, 250 and 50 μM of $NaNO_3$) and Exp. 2) light quality and emersion/immersion (EMER/IMMER) conditions. Values are expressed as mean ± standard deviation (SD) ($n = 3$). Different letters indicate significant differences among treatments: lower-case letters indicate significant interaction between variables (radiation and nutrients or radiation and emersion/immersion), capital letters indicate significant differences between radiation treatments (PAR and $PAR_{UVAViBl+}$) and italic letters indicate significant differences among nutrients concentrations (50, 250 and 500) or emersion/immersion conditions (EMER and IMMER). ANOVA, Newman-Keuls post hoc ($p < 0.05$).

Table 3
Parameters obtained from the rapid light curves (RLCs) measured at day 7 of both experiments with *Pyropia leucosticta*: Exp. 1) light quality and nutrients (500, 250 and 50 μM of $NaNO_3$) and Exp. 2) light quality and emersion/immersion conditions. Maximal quantum yield (F_v/F_m), maximal electron transport rate (ETR_{max}), photosynthetic efficiency of ETR versus Irradiance (α_{ETR}) and saturated irradiance of ETR (Ek_{ETR}). Values are expressed as mean ± standard deviation (SD) ($n = 3$). Different letters indicate significant differences among treatments: lower-case letters indicate significant interaction between variables (radiation and nutrients or radiation and emersion/immersion), capital letters indicate significant differences between radiation treatments (PAR and $PAR_{UVAViBl+}$) and italic letters indicate significant differences among nutrients concentrations (50, 250 and 500) or emersion/immersion conditions (EMER and IMMER). ANOVA, Newman-Keuls post hoc ($p < 0.05$). Asterisk (*) showed significant differences between initial values and the obtained in the different treatments. Student's *t*-test ($p < 0.05$).

		F_v/F_m	ETR_{max}	α_{ETR}	Ek_{ETR}
Exp.1	Initial	0.65 ± 0.05	3.83 ± 1.07	0.03 ± 0.01	129.29 ± 19.89
	PAR 500	0.70 ± 0.01^{c}	3.03 ± 0.48^{b}	0.02 ± 0.00	139.94 ± 23.62
	PAR 250	0.66 ± 0.01^{b}	2.82 ± 0.73^{ab}	0.03 ± 0.01	110.73 ± 4.34
	PAR 50	0.66 ± 0.03^{b}	2.30 ± 0.15^{a*}	0.02 ± 0.01	103.09 ± 25.82
	$PAR_{UVAViBl+}$ 500	0.66 ± 0.01^{b}	2.92 ± 0.31^{b}	0.03 ± 0.01	122.11 ± 41.82
	$PAR_{UVAViBl+}$ 250	0.64 ± 0.01^{b}	2.17 ± 0.36^{ab*}	0.02 ± 0.01	109.86 ± 42.38
	$PAR_{UVAViBl+}$ 50	0.56 ± 0.03^{a**}	2.01 ± 0.32^{a*}	0.03 ± 0.00	79.28 ± 4.55*
Exp.2	Initial	0.67 ± 0.01	3.95 ± 0.42	0.03 ± 0.00	128.76 ± 8.68
	PAR EMER	0.69 ± 0.01*	3.08 ± 0.42	0.03 ± 0.00	112.16 ± 8.68*
	PAR IMMER	0.69 ± 0.02	2.64 ± 0.87	0.02 ± 0.00*	132.15 ± 54.27
	$PAR_{UVViBl+}$ EMER	0.68 ± 0.02	2.60 ± 0.20*	0.02 ± 0.01	135.34 ± 54.50
	$PAR_{UVAViBl+}$ IMMER	0.68 ± 0.02	2.57 ± 0.75*	0.02 ± 0.01	122.40 ± 19.38

observed in certain cases, e.g. F_v/F_m value in the PAR EMER treatment showed a significant increased, the ETR_{max} value showed a significant decrease in the $PAR_{UVAViBl+}$ IMMER treatment, or the Ek_{ETR} showed a significant decreased in the PAR EMER treatment.

Table SM.2 show the ETR, the energy dissipation rate (EDR), and the non-photochemical quenching (NPQ) obtained during RLCs at 75, 150 and 300 μmol photons m^{-2} s^{-1}. In general, a higher EDR than ETR is observed in all treatments of both experiments (e.g. in the PAR 500 treatment at 150 μmol photons m^{-2} s^{-1}, the ETR and EDR values were 2.5 and 8.5, respectively), and the values of the three variables increased with the increasing irradiances (e.g. in the PAR 500 treatment at 150 μmol photons m^{-2} s^{-1}, the ETR values increased from 1.3 to 3.0, the EDR values increased from 3.5 to 19.0 μmol photons m^{-2} s^{-1}, and the NPQ values increased from 0.5 to 0.9). In the first experiment, ETR and EDR only showed significant differences among the different nutrient concentrations at 150 and 300 μmol photons m^{-2} s^{-1}, (no interaction between factors; Table SM.3). Higher ETR values were observed in the treatments with high nitrogen than in the treatments with low nitrogen (e.g. at 300 μmol photons m^{-2} s^{-1} ETR values varied from 3.03 to 1.98 μmol e^{-} m^{-2} s^{-1}). The opposite occurs with the EDR, higher values were obtained in the treatments with low nitrogen (e.g. at 300 μmol photons m^{-2} s^{-1}, the EDR values varied from 20.1 to 19.0 μmol photons m^{-2} s^{-1}). In relation to NPQ values, a significant effect of the radiation treatments was observed for the three light irradiances (no significant interaction between factors; Table SM.3). Higher NPQ values were observed in $PAR_{UVAViBl+}$ treatment than that under PAR treatments (e.g. at 300 μmol photons m^{-2} s^{-1}, the NPQ was 0.83 under PAR treatment and 1.27 under $PAR_{UVAViBl+}$). In the second experiment, ETR and EDR values showed significant effects related to the radiation treatments at 150 μmol photons m^{-2} s^{-1} (Table SM.4). ETR values were higher in the PAR treatment (2.4 μmol e^{-} m^{-2} s^{-1}), than in the $PAR_{UVAViBl+}$ treatment (1.7 μmol e^{-} m^{-2} s^{-1}). The NPQ values did not shown significant differences among treatments (e.g. at 150 μmol photons m^{-2} s^{-1}), the average NPQ were 0.74. The ratio ETR/EDR at different irradiances in the RLCs are shown in Fig. 3. In general, the ratio decreased with the increasing irradiance (e.g. in the PAR 500 treatment the ratio varied from 0.36 to 0.16). In the first experiment, significant effect of the nutrient concentration was observed under 150 and 300 μmol photons m^{-2} s^{-1} (no significant differences were obtained for 75 μmol photons m^{-2} s^{-1}). The highest ratio was observed with the highest nitrogen level (500), and the lowest ratio with the lowest nitrogen (50) (e.g. at 300 μmol photons m^{-2} s^{-1}), decreasing the ratio from 0.16 to 0.11. In the second experiment, significant differences between the radiation treatments were only observed at 150 μmol photons m^{-2} s^{-1}, lower values were observed in the $PAR_{UVAViBl+}$ treatments (0.19) than in the PAR treatment (0.3).

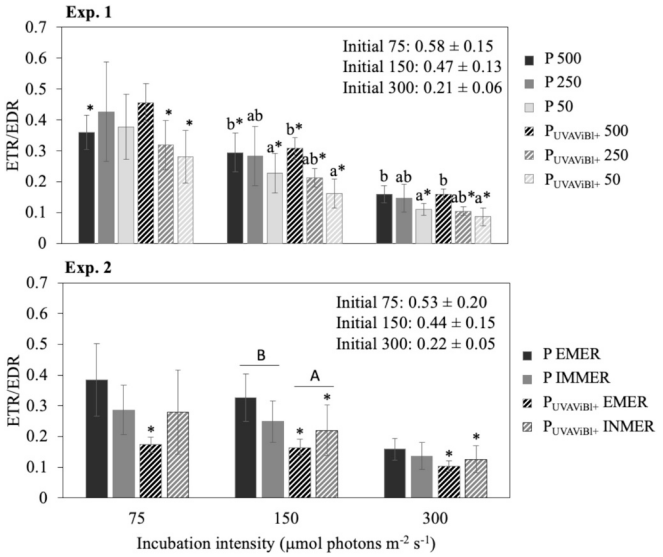

Fig. 3. Ratio between the electron transport rate (ETR) and the electron dissipation rate (EDR) obtained from the rapid light curves (RLCs) at 75, 150 and 300 μmol photons m^{-2} s^{-1} of both experiments with *Pyropia leucosticta*: Exp. 1) light quality and nutrients (500, 250 and 50 μM of $NaNO_3$) and Exp. 2) light quality and emersion/immersion (EMER/IMMER) conditions. Values were expressed as mean ± standard deviation (SD) ($n = 3$). Different letters indicate significant differences among treatments: lower-case letters indicate significant interaction between variables (radiation and nutrients or radiation and emersion/immersion), capital letters indicate significant differences between radiation treatments (PAR and $PAR_{UVAViBl+}$) and italic letters indicate significant differences among nutrients concentrations (50, 250 and 500) or emersion/immersion conditions (EMER/IMMER). ANOVA, Newman-Keuls post hoc ($p < 0.05$).

3.3. Microscopic analysis

Microscopic images of *P. leucosticta* thalli at the end of the experimental period are shown in Fig. 4. Clear spaces represent cell wall while internal content of each cell is colored. Some groups of small cells derived from mitotic division can be observed in all images. In general, the thalli remained with a red-brownish color. In the treatment with high N and only PAR, the red color was more patent, whereas in the treatment with low N and UVR, the color changed to yellowish (Fig. 4).

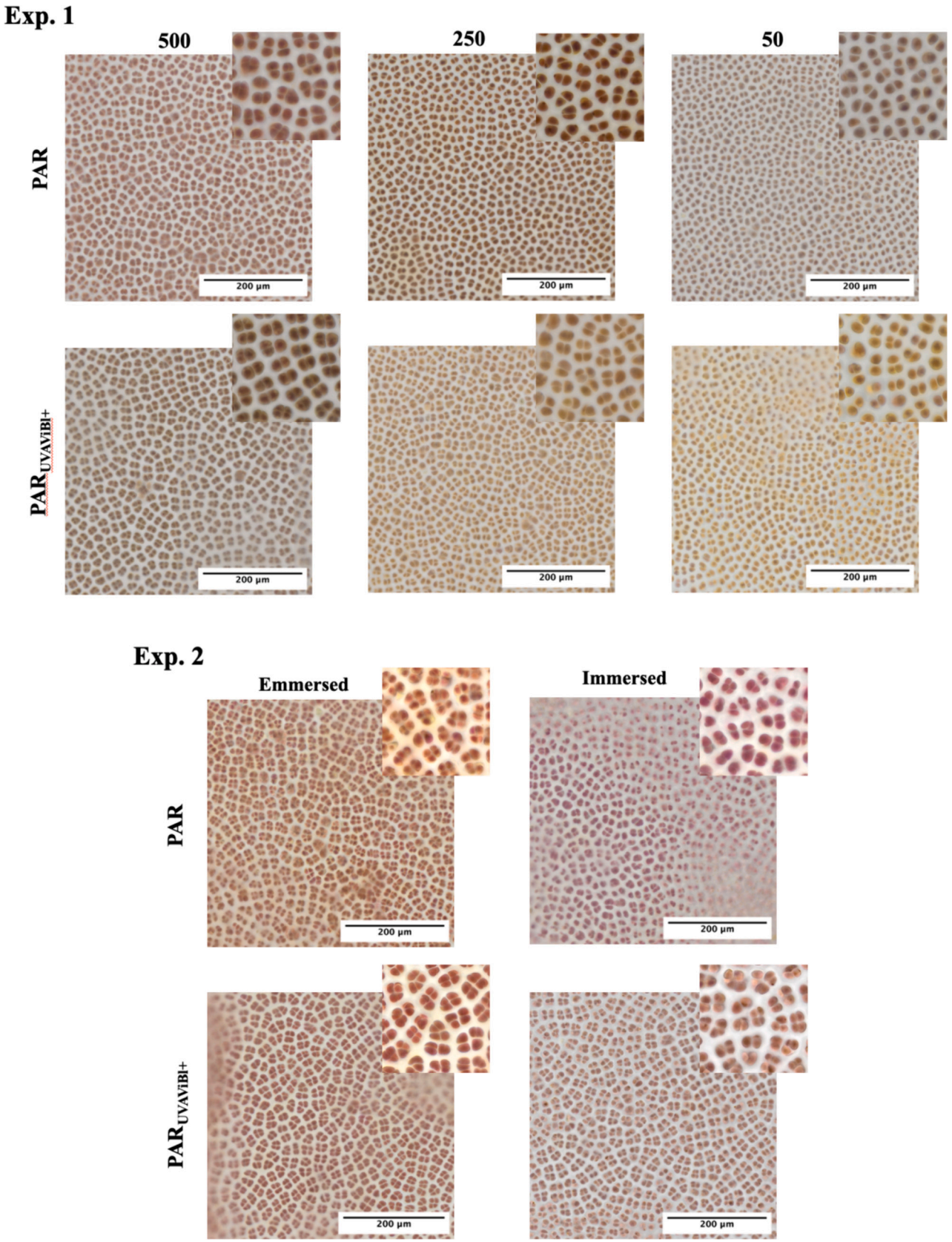

Fig. 4. Microscopic photos of *Pyropia leucosticta* thalli at the end of the experimental period (day 7) for both experiments: Exp. 1) light quality and nutrient concentrations (500, 250 and 50 µM of $NaNO_3$); and Exp. 2) Light quality and emersion/immersion (EMER/IMMER) conditions. Images are representatives of a total of 3 analyzed samples (3 images were performed of each sample).

Different parameters were calculated from those photos: number of cells in the analyzed area, percentage of the protoplasmatic area and average size of the protoplasm (Table 4). In the first experiment, the cell number showed a significant effect of both studied factors separately (Table SM.3). The number of cells were higher in the treatments with low nitrogen, i.e. the cell content varied from 147.6 in the high nitrogen treatment to 253.3 in the low nitrogen content. The cell number was also affected by the $PAR_{UVAiBl+}$ radiation, i.e. lower number was obtained in the $PAR_{UVAViBl+}$ treatment (182.0) than in the PAR treatments (213.2). The protoplasmatic area and the protoplasm size showed interaction between the analyzed factors. The lowest protoplasmatic area (34.9 %) was observed in PAR 50, PAR 250 and $PAR_{UVAViBl+}$ 50 treatments, the other treatments showed an area of 40.0 %. In the case of the protoplasm size, the lowest value was obtained in the $PAR_{UVAViBl+}$ 50 treatment (15.0 μm), and the highest in the PAR 500 treatment (26.0 μm). In relation to the second experiment, significant effect of the radiation treatment was observed in the cell number and in the protoplasm size, whereas the protoplasmatic area was affected by desiccation (Table SM.4). The number of cells increased under $PAR_{UVAViBl+}$ treatments (159.2 vs 183.6). The protoplasmatic area increased under desiccation (38.6 vs 35.18). The protoplasma size decreased under $PAR_{UVAViBl+}$ (32.69 vs 25.51).

3.4. Biochemical analysis

Table 5 show elemental carbon, nitrogen and sulphur contents and the radio C/N. In the first experiment, the carbon content only showed significant differences between radiation treatments in the day 7 (Table SM.3). Lower carbon values were obtained in the $PAR_{UVAViBl+}$ treatments (32.9 %) in comparison to PAR treatments (34.25 %). At day 2, no significant differences were observed among treatments although the carbon content increased in most of the treatment in comparison with the initial values. At day 7, only the PAR 500 treatment showed a significant increase compared to the initial value. In relation to the N content, a separately effect of nutrients concentration and radiation treatment was obtained in day 2 (Table SM.3). The highest nitrogen content was obtained in the treatment with highest nutrient level (500; 2.76 %) and in the P treatments (2.42 %). At day 7, significant effects were observed among the nutrient concentrations (same as day 2) (Table SM.3). An increase of the N content in comparison with the initial value were observed in all treatments. The C/N ratio was also affected by the nutrient concentration in both days (Table SM.3), the lowest ratio was obtained in the treatments with highest nutrient availability. Considering the sulphur content of algal thalli, no significant differences were found (Table SM.3). In relation to the second experiment, the carbon, nitrogen and sulphur content showed a significant interaction between variables (Table SM.4), and the lower C value was obtained in the PAR $_{UVAViBl+}$ -IMMER treatment (29.7 %) and higher in P IMMER treatment (35.8 %). The lowest N-value was obtained in $PAR_{UVAViBl+}$-IMMER treatment (2.5 %) and the highest at PAR IMMER treatment (3.9 %). The C/N ratio only showed significant effect of the radiation treatments (Table SM.4), where higher values was obtained in the $PAR_{UVAViBl+}$ treatments (11.6) in comparison to P treatments (9.7). The highest sulphur value was obtained in PAR- IMMER treatment (1.2 %) and the lowest in $PAR_{UVAViBl+}$-IMMER treatment (0.2 %).

Table 6 show the concentration of phenolic compounds and the antioxidant capacity measured through two different radical scavenging methods (ABTS and DPPH). The phenols content showed a significant effect of the radiation treatments at day 2 (Table SM.3). Higher value was obtained in the $P_{UVA+BLUE}$ treatments (11.9 mg g^{-1} DW) than in the P treatments (9.0 mg g^{-1} DW). However, at day 7 a significant effect of the nutrient concentrations was obtained (Table SM.3). Lowest values were obtained in the treatment with lowest nutrient concentration (50; 9.5 mg g^{-1} DW). The antioxidant capacity measured through ABTS method, showed significant effects of the nutrient concentration at day 2 and radiation treatments at day 7 (Table SM.3). At day 2, highest values were obtained in the intermediate content of nutrients (250; 23.9 μmol TE g^{-1} DW) and in day 7 higher values was obtained in the P treatments (22.2 μmol TE g^{-1} DW) than in the $PAR_{UVAViBl+}$ treatments (16.8 μmol TE g^{-1} DW). The antioxidant capacity through the DPPH methods only showed a significant effect of the light treatments at day 2 (Table SM.3), in which higher values was obtained under $PAR_{UVAViBl+}$ treatments (11.5 μmol TE g^{-1} DW) than under P treatments (6.5 μmol TE g^{-1} DW). In the second experiment, the phenolic compounds and DPPH antioxidant capacity only showed a significant effect of the radiation treatments at day 7 (Table SM.3). In the case of phenolics, a higher content was found in algae under PAR + UVAVB treatments (15.8 mg g^{-1} DW) than under P treatments (13.7 mg g^{-1} DW). The ABTS did not show significant differences (Table SM.3).

Photosynthetic pigments of *P. leucosticta* submitted to the two experimental procedures are shown in Fig. 5. In case of the first experiment, pigments clearly increased during the experimental process and showed a variation caused by significant effects due to nutrient concentrations applied during the experiment (Table SM.3). The values increased with the increasing nutrient concentrations. For phycoerythrin and phycocyanin content, a significant effect of the nutrient concentrations was observed for day 2, whereas at day 7 a significant effect of the radiation treatments was also observed (Table SM.3). At day 2, values of phycoerythrin varied from 4.3 to 11.1 mg g^{-1} DW. At day 7, $PAR_{UVAViBl+}$ showed lower values than PAR treatments (6.1 and 8.2 mg g^{-1} DW, respectively). In the case of chlorophyll *a* (Chl *a*) content, a significant effect of the nutrients was obtained in both days (Table SM.3). The content varied from 1.3 to 2.0 mg g^{-1} DW at day 2. In the second experiment, a significant effect of radiation treatments was only observed for phycoerythrin content at day 7, in which a lower content was obtained in the $PAR_{UVAViBl+}$ (18.2 mg g^{-1} DW) treatments in comparison with PAR treatments (24.7 mg g^{-1} DW). The other two pigments remained constant, although the Chl *a* showed a significant increase in comparison with the initial values.

Finally, the MAA contents of *P. leucosticta* are shown in Fig. 6. In both experiments, the content of MAAs increased throughout the time. In case

Table 4
Parameters measured from microscopic images obtained at the end of the experimental period in both experiments with *Pyropia leucosticta*: Exp. 1) light quality and nutrient concentrations (500, 250 and 50 μM of $NaNO_3$); and Exp. 2) light quality and emersion/immersion (EMER/IMMER) conditions. Number of cells present in the analyze area, protoplasmatic area (%) and protoplasm average size (μm^2). Values are expressed as mean ± standard deviation (SD) ($n = 3$). Different letters indicate significant differences among treatments: lowercase letters indicate significant interaction between variables (radiation and nutrients or radiation and emersion/immersion), capital letters indicate significant differences between radiation treatments (PAR and $PAR_{UVAViBl+}$) and italic letters indicate significant differences among nutrients or emersion/immersion conditions (EMER/IMMER). ANOVA, Newman-Keuls post hoc ($p < 0.05$).

	Treatment	n° cells	Protoplasmatic area (%)	Protoplasmatic average size (μm^2)
Exp. 1	PAR 500	165.89 ± 2.34^{aB}	40.49 ± 2.22^{b}	26.00 ± 2.28^{d}
	PAR 250	202.78 ± 32.67^{bB}	33.65 ± 2.24^{a}	18.24 ± 3.31^{c}
	PAR 50	271.06 ± 27.92^{cB}	32.01 ± 2.38^{a}	12.70 ± 0.60^{a}
	$PAR_{UVAViBl+}$ 500	129.25 ± 1.21^{aA}	39.74 ± 0.17^{b}	32.85 ± 0.30^{c}
	$PAR_{UVAViBl+}$ 250	181.06 ± 25.09^{bA}	38.77 ± 2.31^{b}	22.82 ± 4.43^{b}
	$PAR_{UVAViBl+}$ 50	235.44 ± 24.74^{cA}	32.17 ± 1.45^{a}	15.02 ± 1.02^{ab}
Exp. 2	PAR EMER	113.50 ± 2.00^{A}	37.57 ± 2.31^{ab}	34.28 ± 2.24^{bB}
	PAR IMMER	134.50 ± 10.17^{A}	36.91 ± 1.46^{ab}	29.69 ± 2.25^{aB}
	$PAR_{UVAViBl+}$ EMER	163.11 ± 17.02^{B}	39.72 ± 0.75^{b}	26.39 ± 2.04^{bA}
	$PAR_{UVAViBl+}$ IMMER	154.75 ± 12.25^{B}	35.02 ± 0.23^{a}	24.85 ± 1.61^{aA}

Table 5
Total internal carbon, nitrogen and sulphur content (%), and C/N ratio of both experiments with *Pyropia leucosticta*: A) light quality and nutrient concentrations (500, 250 and 50 μM of $NaNO_3$); and B) light quality and emersion/immersion (EMER/IMMER) conditions. Values are expressed as mean ± standard deviation (SD). Different letters indicate significant differences among treatments: lower-case letters indicate significant interaction between variables (radiation and nutrients or radiation and emersion/immersion), capital letters indicate significant differences between radiation treatments (PAR and $PAR_{UVAViBl+}$), italic letters indicate significant differences among nutrients concentrations or emersion/immersion (EMER/IMMER conditions. ANOVA, Newman-Keuls post hoc ($p < 0.05$). Asterisks (*) indicate significant differences between initial values and the obtained in the different treatments by Student's *t*-test ($p < 0.05$).

	Treatment	C		N		C/N		S	
Exp. 1	Initial	33.02 ± 0.59		1.65 ± 0.23		20.3 ± 2.99		1.08 ± 0.19	
		Day 2	Day 7	Day 2	Day 7	Day 2	Day 7	Day 2	Day 7
	PAR 500	35.92 ± 1.55*	35.14 ± 0.29^{B}*	2.99 ± 0.09^{Bb}*	2.88 ± 0.29^{b}*	12.03 ± 0.28^{a}*	12.31 ± 1.35^{a}*	1.47 ± 0.3	1.18 ± 0.19
	PAR 250	35.46 ± 0.28*	33.86 ± 0.38^{B}	2.23 ± 0.08^{Bb}*	2.41 ± 0.56^{ab}*	15.92 ± 0.47^{b}*	14.69 ± 3.96^{a}	1.27 ± 0.12*	1.08 ± 0.20
	PAR 50	37.65 ± 0.65*	33.76 ± 1.02^{B}	2.03 ± 0.01^{Ba}*	2.23 ± 0.70 ^{a}	18.54 ± 0.42^{c}	16.22 ± 5.01^{b}	1.32 ± 0.01*	1.14 ± 0.28
	$PAR_{UVAViBl+}$ 500	34.06 ± 2.47	33.37 ± 1.84 ^{A}	2.54 ± 0.27^{Ab}*	2.90 ± 0.36^{b}*	13.57 ± 2.24^{a}*	11.64 ± 1.75^{a}*	1.26 ± 0.33	1.04 ± 0.41
	$PAR_{UVAViBl+}$ 250	35.49 ± 1.63*	32.92 ± 1.02 ^{A}	2.10 ± 0.03^{Ab}*	2.22 ± 0.46^{ab}	16.94 ± 0.81^{b}	15.22 ± 2.88^{a}	1.21 ± 0.21	1.11 ± 0.09
	$PAR_{UVAViBl+}$ 50	35.64 ± 1.72*	32.46 ± 1.93 ^{A}	1.98 ± 0.19^{Aa}*	1.50 ± 0.22^{a}	*18.18* ± 2.38^{c}	21.80 ± 2.22^{b}	1.26 ± 0.38	1.02 ± 0.14
Exp. 2	Initial	31.64 ± 0.61		2.33 ± 0.78		14.64 ± 5.01		0.77 ± 0.09	
		Day 7		Day 7		Day 7		Day 7	
	PAR EMER	32.70 ± 1.34^{ab}		3.26 ± 0.36^{b}		10.09 ± 0.82 ^{A}		0.29 ± 0.15^{a}*	
	PAR IMMER	35.84 ± 2.54^{b}*		3.88 ± 0.05^{b}*		9.25 ± 0.69 ^{A}		1.24 ± 0.31^{b}*	
	$PAR_{UVAViBl+}$ EMER	33.30 ± 2.52^{ab}		3.04 ± 0.87^{b}		11.44 ± 2.47^{B}		0.54 ± 0.62 ^{A}	
	$PAR_{UVAViBl+}$ IMMER	29.67 ± 1.62 ^{A}		2.47 ± 0.25^{a}		11.68 ± 1.10^{B}		0.20 ± 0.21^{a}*	

Table 6
Phenols content (mg g^{-1} DW), and antioxidant capacity measured through ABTS and DPPH method (μmol TE g^{-1} DW) of both experiments with *Pyropia leucosticta*: Exp. 1) light quality and nutrient concentrations (500, 250 and 50 μM of $NaNO_3$); and Exp. 2) light quality and emersion/immersion (EMER/IMMER) conditions. Values are expressed as mean ± standard deviation (SD). Different letters indicate significant differences among treatments: lower-case letters indicate significant interaction between variables (radiation and nutrients or radiation and emersion/immersion), capital letters indicate significant differences between radiation treatments (PAR and $PAR_{UVAViBl+}$), italic letters indicate significant differences among nutrients concentrations or emersion/immersion (EMER/IMMER) conditions. ANOVA, Newman-Keuls post hoc ($p < 0.05$).

		Phenols		ABTS		DPPH	
Exp. 1	Initial	11.6 ± 4.44		23.49 ± 0.69		8.53 ± 0.70	
		Day 2	Day 7	Day 2	Day 7	Day 2	Day 7
	PAR 500	8.73 ± 0.63 ^{A}	9.95 ± 1.13^{a}	17.77 ± 2.06^{a}	23.49 ± 2.97^{B}	7.08 ± 2.81 ^{A}	12.52 ± 1.09*
	PAR 250	9.45 ± 2.23 ^{A}	10.94 ± 1.75^{ab}	23.97 ± 4.9^{b}	21.36 ± 2.18^{B}	8.49 ± 7.49 ^{A}	11.74 ± 4.41
	PAR 50	8.91 ± 0.89 ^{A}	13.22 ± 1.28^{b}	20.90 ± 1.66^{a}*	21.74 ± 3.91^{B}	3.75 ± 1.53 ^{A}*	12.37 ± 2.26*
	$PAR_{UVAViBl+}$ 500	11.6 ± 1.95^{B}	9.09 ± 1.15^{a}	16.30 ± 4.61 ^{a}*	15.18 ± 0.62^{A}	9.64 ± 5.1^{B}	12.59 ± 1.6*
	$PAR_{UVAViBl+}$ 250	11.29 ± 0.49^{B}	10.73 ± 1.56^{ab}	23.84 ± 2.22^{b}	15.17 ± 2.61 ^{A}*	12.13 ± 0.51^{B}	15.61 ± 2.38*
	$PAR_{UVAViBl+}$ 50	12.88 ± 2.08^{B}	10.43 ± 0.87^{b}	18.69 ± 2.51^{a}*	20.23 ± 3.36 ^{A}*	12.87 ± 0.99^{B}	9.92 ± 5.85
Exp. 2	Initial	11.31 ± 2.05		18.6 ± 1.6		2.06 ± 1.40	
		Day 3	Day 7	Day 3	Day 7	Day 3	Day 7
	PAR EMER	8.92 ± 2.93	15.07 ± 1.67 ^{A}	17.98 ± 1.49	20.60 ± 0.66*	7.51 ± 1.94*	11.33 ± 1.70 ^{A}*
	PAR IMMER	11.41 ± 3.44	12.38 ± 1.10 ^{A}*	17.87 ± 4.94	23.36 ± 3.18	5.82 ± 3.35	10.95 ± 1.38 ^{A}*
	$PAR_{UVAViBl+}$ EMER	12.84 ± 5.25	15.72 ± 0.50^{B}*	19.80 ± 3.19	20.98 ± 1.10	6.60 ± 3.95	15.04 ± 1.69^{B}*
	$PAR_{UVAViBl+}$ IMMER	10.10 ± 3.9	15.94 ± 0.99^{B}*	19.35 ± 2.25	21.50 ± 1.77	11.42 ± 6.51*	13.17 ± 7.27^{B}*

of the first experiment, a clear effect of nutrients concentration was obtained (Table SM.3). The content of MAAs increased in the treatments with high N-availability. MAAs content varied from 0.8 to 2.7 mg g^{-1} DW at day 2, and from 3.3 to 6.7 mg g^{-1} DW at day 7. In the second experiment, an interaction among variables was obtained (Table SM.4). In day 3, the highest MAA values was obtained in the $PAR_{UVAViBl+}$ EMER treatment (5.1 mg g^{-1} DW). In the end of the experiment, in day 7, the highest values were obtained in PAR IMMER and $PAR_{UVAViBl+}$ EMER treatments, followed by PAR EMER and $PAR_{UVAViBl+}$ IMMER treatment (9.4, 8.1, 6.7 and 4.3 mg g^{-1} DW, respectively).

3.5. Pearson's correlations

Pearson's correlation analysis for experiments conducted with *P. leucosticta* are shown in table SM.5. In the first experiment, some photosynthetic parameters ($_{int}$ETR, F_v/F_m and ETR_{max}) were positively correlated among them and with most of the internal compounds (N, phenols, PE, PC, Chl *a* and MAAs). Nitrogen content correlated positively with the nitrogenous compounds (PE, PC, Chl *a* and MAAs). Carbon content also showed a positive correlation with the phycobiliproteins content (PE and PE). Antioxidant capacities of algal extracts with DPPH assay were correlated with the phenols content, while those obtained from the ABTS assay were correlated with the PC content. In the second experiment, less significant correlations were found. Carbon content correlate with N and S content, as well as, PE, PC and MAAs. Nitrogen content correlated with the nitrogenous compounds (PE, PC and MAAs) and sulphur content, and correlates negatively with the antioxidant capacity (by DPPH). ABTS assay data showed positive correlation with PE and PC of *P. leucosticta*, while antioxidant capacity estimated by DPPH was positively correlated with phenols.

4. Discussion

Photosynthesis is dependent on irradiance, light quality, and nutrient availability among other variables. Nitrogen assimilation is necessary to produce the proteins involved in photosynthesis (and other processes), while at the same time this process demand ATP and NADPH produced in the photosynthetic electron transport chain. In this study, both maximal quantum yield (F_v/F_m) and electron transport rate (ETR) decreased under low nutrient conditions, clearly related to the lower substrate source for photosynthesis and the inability to synthetize important proteins like photosynthetic pigments that harvest the light. F_v/F_m is an indicator of the physiological state of photosynthetic organism [75] and ETR can be related to productivity [30,76]. Low values

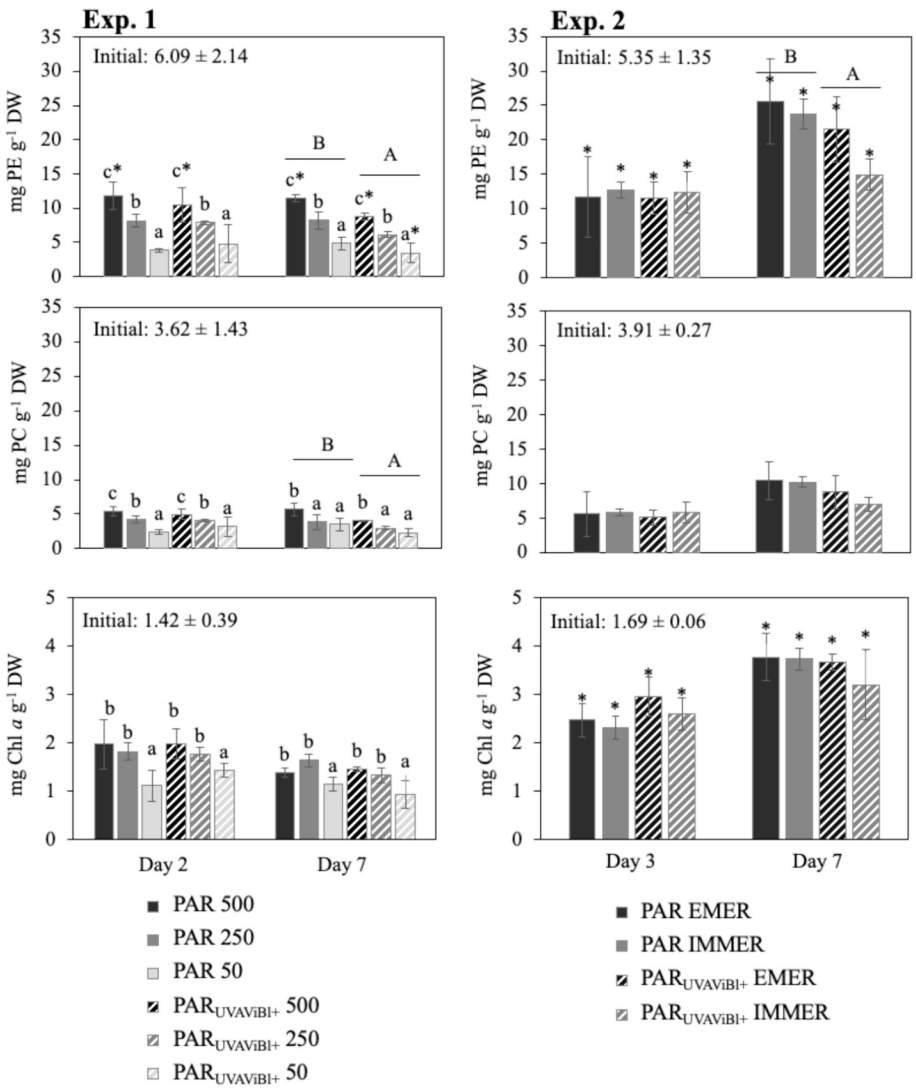

Fig. 5. Photosynthetic pigments (phycoerythrin, phycocyanin and chlorophyll *a*) measured in both experiments with *Pyropia leucosticta*: Exp. 1) light quality and nutrient concentrations (500, 250 and 50 μM of $NaNO_3$) and Exp. 2) light quality and emersion/immersion (EMER/IMMER) conditions. Values are expressed as mean ± standard deviation (SD). Different letters indicate significant differences among treatments: lower-case letters indicate significant interaction between variables (radiation and nutrients or radiation and emersion/immersion), capital letters indicate significant differences between radiation treatments (PAR and $PAR_{UVAViBl+}$), italic letters indicate significant differences among nutrients or emersion/immersion (EMER/INMER) conditions. ANOVA, Newman-Keuls post hoc ($p < 0.05$). Asterisks (*) indicate significant differences between initial values and the obtained in the different treatments. Student's *t*-test ($p < 0.05$).

of both F_v/F_m and ETR are consequence of stress conditions (e.g. low nutrient availability) producing photoinhibition. So, as it is expected, the increase in nitrogen content is related to a high pigment content that allow a higher light absorption, what increase the electron sink and consequently increase the photosynthetic rate [2]. According to the different action spectra showed in fig. SM.2, UV radiation can affect photosynthesis and other processes, through chloroplast inhibition, DNA and proteins damage, or lipid peroxidation. Among them, chloroplast photoinhibition and lipid peroxidation were the most affected by UV-A radiation. This can explain the reduction in the integrated ETR under the $PAR_{UVAViBl+}$ treatment in some cases (e.g. the day 0 or the $PAR_{UVAViBl+}$ 250 at day 7) during the first experiment. However, the interaction between both studied factors (light quality and nutrients) during the experimental period in the F_v/F_m and ETR values, suggest that high nitrogen availability can help to reduce or delay the negative effect provoke by UV-A radiation. This positive effect has been previously reported by Figueroa et al. and Bonomi-Barufi et al. [77–79] in *Ulva lactuca* and *Gracilaria tenuisipitata*, respectively. Additionally, the violet-blue light increased the amount of photons available for photosynthesis [80] in the $PAR_{UVAViBl+}$ treatment, that can explain the significant increase in the ETR_{int} observed in the $PAR_{UVAViBl+}$ 500 at day 2 and 6 and in the algae cultured under $PAR_{UVAViBl+}$ during the first day of the second experiment. This supplemented radiation has a positive effect on photosynthesis only during a short period, whereas the positive effect of high nutrient availability is maintained during a longer time. The photosynthetic increase with the supplemented light can be also due to photomorphogenic responses of these wavelength through the action of cryptochromes as it has been shown by other authors [19,25].

On the other hand, emersed conditions caused a decrease in the photosynthetic capacity ($_{in\ situ}$ETR) after 3 h of emersion, followed by a recovery after the re-hydration (see Fig SM4). This pattern has been observed in different species, such as *Porphyra columbina*, *Mastocarpus papillatus* or *Mazzaella laminarioides* [39,41,81]. Zou and Gao [82] observed that the photosynthetic capacity of *Porphyra haitanensis* decreased under emersion due to limitation of the atmospheric CO_2, demonstrating that higher CO_2 concentrations will enhance the photosynthetic capacity. In contrast, many macroalgae have shown an increase in the photosynthetic rate in moderate emersion conditions, like

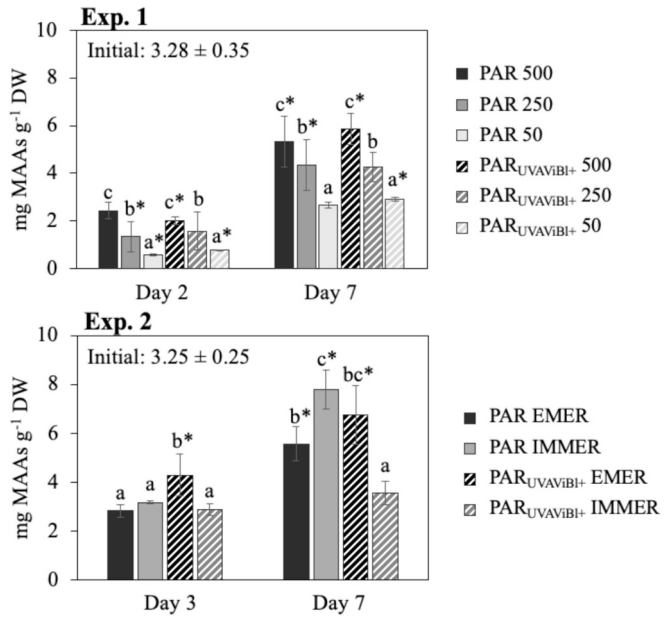

Fig. 6. Mycosporine-like amino acids (MAAs) measured in both experiments with *Pyropia leucosticta*: Exp. 1) light quality and nutrients (500, 250 and 50 μM of $NaNO_3$) and Exp. 2) light quality and emersion/immersion (EMER/INMER) conditions. Values are expressed as mean ± standard deviation (SD). Different letters indicate significant differences among treatments: lower-case letters indicate significant interaction between variables (radiation and nutrients or radiation and emersion/immersion), capital letters indicate significant differences between radiation treatments (PAR and $PAR_{UVAViBl+}$), italic letters indicate significant differences among nutrients or emersion/immersion (EMER/IMMER) conditions. ANOVA, Newman-Keuls post hoc ($p < 0.05$). Asterisk (*) showed significant differences between initial values and the obtained in the different treatments. Student's *t*-test ($p < 0.05$).

Porphyra yezoensis, Ishige okamurae, Chondracanthus intermedius or *Pterocladia capillacea* [40] due to the removal of the water layer on the surface of the thallus and the higher diffusion rate of CO_2 in air than in water (10,000 times higher). Nevertheless, prolonged desiccation periods produce negative effects for photosynthesis due to a further decrease of water content. Water is necessary for the proper function of the photosystem (PS) II and the electron flow between the two photosystems, whereas the cyclic electron flow around PS I do not need water and plays a significant physiological role during desiccation and rehydration, i.e. Gao et al. [83] observed that the cyclic electron flow improve the recovery after severe desiccation in *Porphyra yezoensis*.

The ETR_{max} values determined during RLCs showed a similar pattern that the obtained in the ETR_{int} calculated in situ, although the values were very different. The ETR_{max} values obtained incubating algae under the red LED light of the Mini-PAM (that reach 1200 μmol photons m^{-2} s^{-1}) were much lower than that ETR values obtained in situ at 300 μmol photons m^{-2} s^{-1} of white LED light (3.3 vs 14.8 μmol e^- m^{-2} s^{-1}, respectively in the PAR 500 treatment). These differences have been observed by other species of macroalgae (*Ulva lactuca*, *Ulva rigida* and *Gracilaria cornea*) and microalgae (*Chlorella fusca*) [2,30,76,84]. Figueroa et al. [30] suggested that this difference can be due to the light quality of the incubation light. Solar or white light present a broader spectrum than the red, blue or the white halogen lights of the PAM devices, thus chlorophyll *a* and accessory pigments can absorb light from different wavelengths, reaching a higher photosynthetic capacity.

From the RLCs, it can be observed how much energy is dissipated and in which way. The term energy dissipation rate (EDR), proposed for the first time in this work, is related to the amount of energy that is dissipated and it is calculated using both yield losses: Y(NO) and Y(NPQ), instead of the Y(II) (used for ETR calculation). The dissipation can be performed through two mechanisms: Y(NPQ), that is related with the dissipation as fluorescence and heat through photoregulated mechanisms (e.g. xanthophyll cycle) and Y(NO), that is refer to the passively dissipation as heat and/or fluorescence, mainly due to close PSII reaction centers. In all treatments, most of the obtained energy is dissipated, although differences in the ratio ETR/EDR (production/dissipation) were observed among treatments. The non-photochemical quenching (NPQ) is the ratio between both yield losses (Y(NPQ)/Y(NO)), values higher than 1 indicate that the main dissipation mechanism is the photoregulated one. The results indicate that under high intensities, the ETR/EDR decreased and the NPQ increased, showing that algae are not able to use all the available energy, and as photoprotection mechanism the photoregulated dissipation mechanism increased. The ratio ETR/EDR was affected by nutrient availability as was observed with ETR values since both values are related, i.e. if ETR values decrease, EDR values increased. However, the NPQ was only affected by the $PAR_{UVAViBl+}$ radiation, increasing the values under this type of radiations and indicating that a photorregulated dissipation mechanism is activated under this condition. When emersion and UVA, Violet and Blue were combined, a decrease in ETR/EDR was observed, probably due to the effect of light quality (no effect of the emersion conditions were observed).

Other authors have used the ratio ETR/NPQ as indicator of the relation between energy used on photosynthesis and dissipation quenching [85]. The authors shown that this ratio decreased under increased stress condition, e.g. increase the exposure UV-B radiation. ETR/EDR is suggested as a better indicator than ETR/NPQ since they are expressed in the same energy units and they represent the ratio of energy used for photosynthesis (ETR) and dissipation (EDR). Hendrikson et al. [86] proposed a simpler alternative method for quantifying the partitioning of excitation energy between photochemistry, thermal/fluorescence dissipation or photoregulated dissipation. They calculated the energy used or dissipated as the product between YII, Y(NO) or Y(NPQ) and the absorbed irradiance and expressed it as irradiance unit (μmol photons m^{-2} s^{-1}). Figueroa et al. [2] also calculated the energy used and dissipated but taking into account the absorbed irradiance and the fraction of chlorophyll *a* associated to PSII (F_{II}). The EDR was proposed in this work, as a form to calculate the general energy dissipation, taking into account both yield losses, Y(NO) and Y(NPQ).

In addition to the effects of the different factors on photosynthesis, the microscopic photographs showed that light, nitrate and emersion can induce morphological cell changes. Under low nitrogen conditions the surface/volume (S/V) ratio is estimated to increased (i.e. n° cells increased and the protoplasm average size decreased), what would favor a high nitrogen incorporation [22]. The opposite is observed in algae under $PAR_{UVAViBl+}$ radiation, where the number of cells decreased, and their size increased, what mean a reduction of the S/V ratio. These morphological changes can be attributed to a photoprotection strategy, decreasing potentially the entrance of UV-A radiation in the inner part of the cells. The increase of cell size of *P. leucosticta* under blue light has been previously observed by Figueroa et al. [22], who observed that the content of PE was much higher under blue light than that under red light, although growth rate in term of area was much lower in blue light and consequently the PE productivity decreased. In this work, we also observed a positive correlation between the protoplasm average size and the accumulation of certain compounds like phycoerythrin, phenols or MAAs. It is also expected that UV radiation cause an increase of the intercellular matrix due to the synthesis of carbonated compounds (such as polysaccharides) as protection mechanism to reduce the penetration of UV rays in the cells [87–89], although the obtained results did not show a clear effect of the $PAR_{UVAViBl+}$ radiation on the protoplasmatic area, and the total C content did not increased under these treatments. Emersion condition increased the protoplasm size, that can be a strategy to reduce the S/V ratio, avoiding the water evaporation. As mentioned before, it is expected that under UV radiation the S/V ratio decrease (as it is estimated in the first experiment), but in the second experiment the opposite occurred: the n° cell increase and protoplasm average size

decreased (the S/V ratio is estimated to increase). Escassi et al. [90] observed that the potassium influx into the cells, influenced the thallus area, so the osmotic regulation related to emersed or immersed conditions can interfere in the obtained results.

The total carbon values of 30–35 % are in accordance with the obtained by other authors [91,92], its content showed a little increase in the treatments with only PAR probably due to the major content of several compounds (e.g. biliproteins or phenols). The nitrogen content clearly increased in the treatments with high nitrogen availability. In this study carbon was not enriched and thus C/N increased in the treatment with low nutrients. Stoichiometry imbalance as the increase of C/N from 12.0 in the treatments with 500 μM of nitrate to 18.5 in the treatments under 50 μM nitrate can have negative physiological effects, reducing not only photosynthetic rate but also photoprotection. It is known the role of increased inorganic dissolved carbon on photoprotection due to increase of dissipating excess of light energy [93,94]. It has been observed that desiccation conditions induce nitrogen release, followed by a rapid incorporation during re-hydration [95]. Thomas et al. [96] observed that desiccation appears to enhance the uptake of nitrate and ammonia in four intertidal species (*Pelvetiopsis limitata*, *Fucus distichus*, *Enteromorpha intestinalis* and *Gigartina papillate*), whereas phosphate uptake did not show and enhancement by desiccation [97]. Kim et al. [98] found that *Porphyra* species followed different patterns in the nitrogen recovery during re-hydration depending on the vertical distribution, i.e. species from the upper-littoral showed a very fast recovery, while lower- or sub-littoral species could not recover. Thus, normally species that are subjected to periods of desiccation showed higher internal N content than the others. In the emersion experiment, similar N content was observed among treatments, only immersed algae under $PAR_{UVAViBl+}$ showed a lower content. This can suggest that the emersion could act as a photoprotection mechanism, through a more rapid N incorporation. However, no significant differences among treatments were observed in nitrogen uptake rate.

Algae color changed under the different treatments. Under low nitrogen, thalli become more brownish mainly due to biliproteins degradation. These pigments are considered nitrogen reservoirs, so under low nitrogen conditions, these molecules break down, supplying the lack of nitrogen for the basal metabolism [99]. Biliproteins are very vulnerable to high exposure of PAR and UV radiation, whereas blue light can induce their synthesis and accumulation in the cells [18,19]. In this work, the combination of Violet-Blue light with UVA radiation seems to reduce or delay the negative effect of the UV-A radiation on the phycobiliproteins content, as a slight significant effect of the radiation treatment was only observed after 7 days of culture.

Generally, the content of bioactive compounds (phenols, MAAs and phycobiliproteins) are correlated with the photosynthetic activity (ETR_{int} and ETR_{max}) since a higher amount of energy is available for been used to synthetize new molecules inside the cells. This positive correlation was observed in the first experiment. As polyphenols act as protective agents in algae, it is expected the increment of these molecules under UV radiation. This effect was observed at day 2, although after 7 days of culture, the effect of the radiation disappeared, and the effect of the nitrogen availability became more prominent. Phenols contents increased in the treatment with low nitrogen, nitrogen limitation stimulates the synthesis of C-compounds such as lipids, carotenoids or phenols. Other authors also observed this response, Sharma et al. [100] reviewed the effect of nitrogen starvation in the lipids content from different microalgae species. Lamers et al. [101] also observed carotenoid accumulation in *Dunaliella salina* induced by nutrient limitations.

Mycosporine-like amino acids (MAAs) clearly increased with high nitrogen availability as it has been previously described in red algae, including *Porphyra* species [28,29,102] with variations along the culture time [30,102,103]. UV-A radiation stimulates the accumulation of MAAs [19,25,28,30,103,104], although in this study no differences between PAR and $PAR_{UVAViBl+}$ treatments were observed when was combined with different nutrients levels. The emersion condition seems to stimulate the synthesis of MAAs in combination with $PAR_{UVAViBl+}$ radiation at day 3. However, at day 7 the content of MAAs increased in all treatments except in the $PAR_{UVAViBl+}$ IMMER. Thus, the $PAR_{UVAViBl+}$ seems to inhibit the accumulation of these molecules under immersion, contrary to the emersion condition. As the emersion can lead to higher PAR and nitrogen starvation, this difference can be related with the lowest N content in this treatment. There is very few information about the effect of emersion/immersion conditions in the MAAs content. Jian et al. [105] submitted *P. haitanensis* acclimated to laboratory culture conditions (no UV radiation and no emersion) to full solar radiation and desiccation conditions, and observed an increase of UV-absorbing compounds in the specimens that were submitted to desiccation, without effect of the UV radiation.

A difference between this and other studies that observed MAAs stimulation with UV radiation, is that we have used a LED of UV-A radiation with maximal emissions at 365 nm in combination with the Q-panel fluorescent lamp. Previous works only used the Q-Panel lamp with maximal emission at 340 nm and with small content of UV-B (in this work we cut off the UV-B), closer to the maximal absorptions of MAAs and maybe can stimulate more optimally the synthesis of MAAs. However, Huang et al. [106] increased the level of fucoxanthin and MAAs in two microalgae (*Nitzschia closterium* and *Isochrysis zhangjiangensis*) using a UV-A light with maximum absorption at 365 nm. Another explanation is that *P. leucosticta* is an alga that live in a very stressful environment and normally present a high constitutive content of MAAs in nature [107], that probably need higher radiation doses or more intense desiccation events.

Regarding the antioxidant capacity, both methodologies used are based on the free-radical scavenging capacity, although there are some differences between them. ABTS is a water-soluble reagent, so it is used for the analysis of hydrophilic compounds such as biliproteins, proteins or polysaccharides, whereas DPPH is only soluble in organic solvents (e.g. methanol, ethanol, chloroform or hexane) and can measured apolar compounds such as phenols, lipids or chlorophylls. In this work the ABTS correlated with phycobiliproteins content and DPPH with phenols content. The antioxidant capacity is considered a protection mechanism against stressful conditions (where there are ROS production) [108], although in this work the $PAR_{UVAViBl+}$ treatments only provoke a small increase in the DPPH antioxidant capacity at day 2 for the nutrients experiments and at day 7 for emersion experiment. Other authors have observed an increase in the antioxidant capacity (measured through the ABTS method) in three red algae (*Gracilaria cornea*, *Gracilariopsis longissima* and *Halopithys incurva*) culture under UV radiation in comparison algae culture under only PAR [103].

No effect of the emersion/immersion conditions in the antioxidant capacity were observed. Contreras-Porcia et al. [39] observed an increase of ROS production and antioxidant enzymes (e.g. catalase (CAT), ascorbate peroxidase (AP) and glutathione reductase (GR)) during emersion, followed by a decrease to normal values during re-hydration. As mentioned before, as *Porphyra* sensu lato species are used to live in stressful environments, it would be necessary a higher intensity or doses of the light treatments and a stronger desiccation to observed differences. In relation to emersion, other authors worked with more patent desiccation, as they achieve values of F_v/F_m close to 0 [39].

In nature, algae a submitted to an interaction of those analyzed factors. Multifactorial or in the field experiments would be necessary to study interactions among them. However, multifactorial experiments in laboratory control conditions could be difficult to performed, as it required a lot of material, space and enough personal to carried out all the measurements. The high nitrogen availability clearly increased the content of nitrogenous compounds and normally improve the physiological state of algae (ref). As emersion condition seems to stimulate the incorporation of N (ref), its combination with different nitrogen concentrations would be interesting. In addition, during emersion algae are exposed to a high solar radiation. However, it would be necessary to

achieve a more drastic desiccation conditions to observe better responses (as it can be observed in nature, where *Porphyra* can be complete dry).

The stimulation of certain compounds in a short period (2–7 days) can be a strategy to increase the productivity of interesting molecules with potential applications during culture. In addition to the food use, *Porphyra* sensu lato species present a high interest for cosmeceutical application, mainly due to the high content of MAAs, that provide photoprotection capacity, as well as antioxidant or anti-aging properties [17,49]. One of the limitations for the use of *Porphyra* sensu lato as cosmeceutic ingredient in that the obtained biomass is preferably used for human consumption. The stimulation of the production of high-added value compounds, such as MAAs, for the cosmeceutic industry can be a way to diversify the industrial use of *Porphyra* sensu lato.

5. Conclusions

In conclusion, the short-term stressed conditions studied in this work can modify the biochemical composition of *P. leucosticta*, maintaining the photosynthetic capacity. The effects of the combination of UV-A (320–400 nm with a peak at 365 nm), and violet-blue light (400–500 nm) is studied for the first time in this work. The nitrogen availability clearly increased the content of nitrogenous compounds and enhance the physiological state of algae. The interactive effect of UVA-Violet-Blue radiation and nutrients concentration suggested that the high nutrient availability play an important role in photoprotection against the UV-A radiation. In general, the combination of UVA-Violet and Blue light showed small effects. It has been observed that the violet-blue light could reduce or delay the negative effect of UV-A radiation in photosynthesis due the accumulation of photoprotectors with antioxidant capacity. The term electron dissipation rate (EDR) and the ratio ETR/EDR are described for the first time in this work, as a way to know the amount of energy used in photochemistry and dissipated. The emersion was not very drastic in this experiment, but some patterns can be observed. Algae were able to recover after 4 h of emersion. Under a short period the UVA-violet-blue radiation and emersion condition seem to increase the MAAs content. The studied stressed conditions could be scaled up in inland culture facilities, and the supplementation of violet-blue light can be used as a way to minimize the negative effects caused by solar radiation.

CRediT authorship contribution statement

Julia Vega: Writing – review & editing, Writing – original draft, Methodology, Investigation, Formal analysis, Conceptualization. **Bruna R. Moreira:** Writing – review & editing, Methodology, Investigation. **Antonio Avilés:** Writing – review & editing, Methodology, Formal analysis. **José Bonomi-Barufi:** Writing – review & editing, Writing – original draft, Supervision, Investigation, Formal analysis. **Félix L. Figueroa:** Writing – review & editing, Writing – original draft, Supervision, Resources, Project administration, Methodology, Investigation, Funding acquisition, Formal analysis, Conceptualization.

Declaration of competing interest

Authors declare no conflict of interest.

Data availability

Data will be made available on request.

Acknowledgements

This research was funded by the Junta de Andalucia (Spain) (Project Blue nutricosmeceutics with cyanobacteria and algae; NAZCA, PY20-00458) and the Ministry of Science and Innovation of Spain (ALGA-HUB project; TED2021-131555B-C22). The authors thank the technical support of Dr. Marta García Sánchez and Yasmín Carvajal Marmoucha during the experiments.

Appendix A. Supplementary data

Supplementary data to this article can be found online at https://doi.org/10.1016/j.algal.2024.103555.

References

[1] F. Lalegerie, L. Gager, V. Stiger-Pouvreau, S. Connan, The stressful life of red and brown seaweeds on the temperate intertidal zone: effect of abiotic and biotic parameters on the physiology of macroalgae and content variability of particular metabolites, Adv. Bot. Res. (2020) 247–287, https://doi.org/10.1016/bs.abr.2019.11.007.

[2] F.L. Figueroa, J. Bonomi-Barufi, P.S.M. Celis-Plá, U. Nitschke, F. Arenas, S. Connan, M.H. Abreu, E.-J. Malta, R. Conde-Álvarez, F. Chow, M.T. Mata, O. Meyerhoff, D. Robledo, D.B. Stengel, Short-term effects of increased CO2, nitrate and temperature on photosynthetic activity in *Ulva rigida* (Chlorophyta) estimated by different pulse amplitude modulated fluorometers and oxygen evolution, J. Exp. Bot. 72 (2021) 491–509, https://doi.org/10.1093/jxb/eraa473.

[3] M. Rezayian, V. Niknam, H. Ebrahimzadeh, Oxidative damage and antioxidative system in algae, Toxicol. Rep. 6 (2019) 1309–1313, https://doi.org/10.1016/J.TOXREP.2019.10.001.

[4] D.B. Stengel, S. Connan, Marine Algae: A Source of Biomass for Biotechnological Applications, Humana Press, New York, NY, 2015, pp. 1–37, https://doi.org/10.1007/978-1-4939-2684-8_1.

[5] N. Nunes, S. Ferraz, S. Valente, M.C. Barreto, M.A.A. Pinheiro de Carvalho, Biochemical composition, nutritional value, and antioxidant properties of seven seaweed species from the Madeira archipelago, J. Appl. Phycol. 29 (2017) 2427–2437, https://doi.org/10.1007/S10811-017-1074-X/TABLES/5.

[6] J. Olsson, G.B. Toth, E. Albers, Biochemical composition of red, green and brown seaweeds on the Swedish west coast, J. Appl. Phycol. 32 (2020) 3305–3317, https://doi.org/10.1007/S10811-020-02145-W/FIGURES/1.

[7] R.R. Sonani, R.P. Rastogi, R. Patel, D. Madamwar, Recent advances in production, purification and applications of phycobiliproteins, World J. Biol. Chem. 7 (2016) 100, https://doi.org/10.4331/WJBC.V7.I1.100.

[8] H. Chen, H. Qi, P. Xiong, H. Chen, H. Qi, P. Xiong, Phycobiliproteins - a family of algae-derived biliproteins: productions, characterization and pharmaceutical potentials, Mar. Drugs 20 (2022) 450, https://doi.org/10.3390/MD20070450.

[9] M. Zubia, D. Robledo, Y. Freile-Pelegrin, Antioxidant activities in tropical marine macroalgae from the Yucatan Peninsula, Mexico, J. Appl. Phycol. 19 (2007) 449–458, https://doi.org/10.1007/s10811-006-9152-5.

[10] P.A. Tenorio-Rodriguez, J.I. Murillo-Álvarez, Á.I. Campa-Cordova, C. Angulo, Antioxidant screening and phenolic content of ethanol extracts of selected Baja California Peninsula macroalgae, J. Food Sci. Technol. 54 (2017) 422–429, https://doi.org/10.1007/S13197-016-2478-3/FIGURES/4.

[11] N. Heffernan, T.J. Smyth, R.J. Fitzgerald, A. Soler-Vila, N. Brunton, Antioxidant activity and phenolic content of pressurised liquid and solid–liquid extracts from four Irish origin macroalgae, Int. J. Food Sci. Technol. 49 (2014) 1765–1772, https://doi.org/10.1111/IJFS.12512.

[12] M. Guinea, V. Franco, L. Araujo-Bazán, I. Rodríguez-Martín, S. González, In vivo UVB-photoprotective activity of extracts from commercial marine macroalgae, Food Chem. Toxicol. 50 (2012) 1109–1117, https://doi.org/10.1016/J.FCT.2012.01.004.

[13] J. Cotas, A. Leandro, P. Monteiro, D. Pacheco, A. Figueirinha, A.M.M. Gonçalves, G.J. Da Silva, L. Pereira, Seaweed phenolics: from extraction to applications, Mar. Drugs 18 (2020) 384, https://doi.org/10.3390/MD18080384.

[14] S. Lomartire, J. Cotas, D. Pacheco, J.C. Marques, L. Pereira, A.M.M. Gonçalves, Environmental impact on seaweed phenolic production and activity: an important step for compound exploitation, Mar. Drugs 19 (2021) 245, https://doi.org/10.3390/MD19050245.

[15] N. Wada, T. Sakamoto, S. Matsugo, Mycosporine-like amino acids and their derivatives as natural antioxidants, Antioxidants 4 (2015) 603–646, https://doi.org/10.3390/antiox4030603.

[16] E. Chrapusta, A. Kaminski, K. Duchnik, B. Bober, M. Adamski, J. Bialczyk, Mycosporine-like amino acids: potential health and beauty ingredients, Mar. Drugs 15 (2017) 326, https://doi.org/10.3390/md15100326.

[17] J. Vega, G. Schneider, B.R. Moreira, C. Herrera, J. Bonomi-Barufi, F.L. Figueroa, Mycosporine-like amino acids from red macroalgae: UV-Photoprotectors with potential cosmeceutical applications, Appl. Sci. 11 (2021) 5112, https://doi.org/10.3390/APP11115112.

[18] N. Korbee, F. Figueroa, J. Aguilera, Effect of light quality on the accumulation of photosynthetic pigments, proteins and mycosporine-like amino acids in the red alga Porphyra leucosticta, J. Photochem. Photobiol. 80 (2005) 71–78, https://doi.org/10.1016/j.jphotobiol.2005.03.002.

[19] G. Schneider, F.L. Figueroa, J. Vega, A. Avilés, P. Chaves, P.A. Horta, N. Korbee, J. Bonomi-Barufi, Physiological and biochemical responses driven by different UV-visible radiation in: *Osmundea pinnatifida* (Hudson) Stackhouse (Rhodophyta), Photochem. Photobiol. Sci. 19 (2020) 1650–1664, https://doi.org/10.1039/d0pp00135j.

[20] W. Rüdiger, F. López-Figueroa, Photoreceptors in algae, Photochem. Photobiol. 55 (1992) 949–954, https://doi.org/10.1111/J.1751-1097.1992.TB08542.X.
[21] A. Kianianmomeni, A. Hallmann, Algal photoreceptors: in vivo functions and potential applications, Planta 239 (2014) 1–26, https://doi.org/10.1007/S00425-013-1962-5/FIGURES/9.
[22] F.L. Figueroa, J. Aguilera, F.X. Niell, Red and blue light regulation of growth and photosynthetic metabolism in *Porphyra umbilicalis* (Bangiales, Rhodophyta), Eur. J. Phycol. 30 (1995) 11–18, https://doi.org/10.1080/09670269500650761.
[23] L.A. Franklin, G. Kräbs, R. Kuhlenkamp, Blue light and UV-A radiation control the synthesis of mycosporine-like amino acids in *Chondrus crispus* (Florideophyceae), J. Phycol. 37 (2001) 257–270, https://doi.org/10.1046/j.1529-8817.2001.037002257.x.
[24] J.B. Barufi, F.L. Figueroa, E.M. Plastino, Effects of light quality on reproduction, growth and pigment content of *Gracilaria birdiae* (Rhodophyta: Gracilariales), Sci. Mar. 79 (2015) 15–24, https://doi.org/10.3989/scimar.04049.12A.
[25] A. Ben Ghedifa, J. Vega, N. Korbee, F. Mensi, F.L. Figueroa, S. Sadok, Effects of light quality on the photosynthetic activity and biochemical composition of Gracilaria gracilis (Rhodophyta), J. Appl. Phycol. 33 (2021) 3413–3425, https://doi.org/10.1007/s10811-021-02496-y.
[26] G. Schneider, F.L. Figueroa, J. Vega, A. Avilés, P.A. Horta, N. Korbee, J. Bonomi-Barufi, Effects of UV–visible radiation on growth, photosynthesis, pigment accumulation and UV-absorbing compounds in the red macroalga *Gracilaria cornea* (Gracilariales, Rhodophyta), Algal Res. 64 (2022) 102702, https://doi.org/10.1016/J.ALGAL.2022.102702.
[27] J. Petersen, A. Rredhi, J. Szyttenholm, S. Oldemeyer, T. Kottke, M. Mittag, The world of algae reveals a broad variety of cryptochrome properties and functions, Front. Plant Sci. 12 (2021) 2472, https://doi.org/10.3389/FPLS.2021.766509/BIBTEX.
[28] N. Korbee-Peinado, R.T. Abdala Díaz, F.L. Figueroa, E.W. Helbling, Ammonium and UV radiation stimulate the accumulation of mycosporine-like amino acids in *Porphyra columbina* (Rhodophyta) from Patagonia, Argentina, J. Phycol. 40 (2004) 248–259, https://doi.org/10.1046/j.1529-8817.2004.03013.x.
[29] J.B. Barufi, N. Korbee-Peinado, M.C. Oliveira, F.L. Figueroa, Effects of N supply on the accumulation of photosynthetic pigments and photoprotectors in *Gracilaria tenuistipitata* (Rhodophyta) cultured under UV radiation, J. Appl. Phycol. 23 (2011) 457–466, https://doi.org/10.1007/s10811-010-9603-x.
[30] F.L. Figueroa, F. Álvarez-Gómez, J. Bonomi-Barufi, J. Vega, T.F. Massocato, J. L. Gómez-Pinchetti, N. Korbee, Interactive effects of solar radiation and inorganic nutrients on biofiltration, biomass production, photosynthetic activity and the accumulation of bioactive compounds in *Gracilaria cornea* (Rhodophyta), Algal Res. 68 (2022) 102890, https://doi.org/10.1016/J.ALGAL.2022.102890.
[31] G. Gao, Q. Gao, M. Bao, J. Xu, X. Li, Nitrogen availability modulates the effects of ocean acidification on biomass yield and food quality of a marine crop *Pyropia yezoensis*, Food Chem. 271 (2019) 623–629.
[32] J.B. Barufi, M.T. Mata, M.C. Oliveira, F.L. Figueroa, Nitrate reduces the negative effect of UV radiation on photosynthesis and pigmentation in *Gracilaria tenuistipitata* (Rhodophyta): the photoprotection role of mycosporine-like amino acids, Phycologia 51 (2012) 636–648, https://doi.org/10.2216/10.77.1.
[33] I. Hernández, M.A. Fernández-Engo, J.L. Pérez-Lloréns, J.J. Vergara, Integrated outdoor culture of two estuarine macroalgae as biofilters for dissolved nutrients from *Sparus auratus* waste waters, J. Appl. Phycol. 17 (2005) 557–567, https://doi.org/10.1007/s10811-005-9006-6.
[34] F.L. Figueroa, A. Bueno, N. Korbee, R. Santos, L. Mata, A. Schuenhoff, Accumulation of mycosporine-like amino acids in *Asparagopsis armata* grown in tanks with fishpond effluents of gilthead sea bream, *Sparus aurata*, J. World Aquac. Soc. 39 (2008) 692–699, https://doi.org/10.1111/j.1749-7345.2008.00199.x.
[35] M.H. Abreu, R. Pereira, C. Yarish, A.H. Buschmann, I. Sousa-Pinto, IMTA with *Gracilaria vermiculophylla*: productivity and nutrient removal performance of the seaweed in a land-based pilot scale system, Aquaculture 312 (2011) 77–87, https://doi.org/10.1016/J.AQUACULTURE.2010.12.036.
[36] R. Bermejo, M. Macías, C.L. Cara, J. Sánchez-García, I. Hernández, Culture of *Chondracanthus teedei* and *Gracilariopsis longissima* in a traditional salina from southern Spain, J. Appl. Phycol. 31 (2019) 561–573, https://doi.org/10.1007/s10811-018-1516-0.
[37] D.Y. Ashkenazi, F.L. Figueroa, N. Korbee, M. García-Sánchez, J. Vega, S. Ben-Valid, G. Paz, E. Salomon, Á. Israel, A. Abelson, Enhancing bioproducts in seaweeds via sustainable aquaculture: antioxidant and sun-protection compounds, Mar. Drugs 20 (2022) 767, https://doi.org/10.3390/MD20120767/S1.
[38] L. Contreras-Porcia, C. López-Cristoffanini, A. Meynard, M. Kumar, Tolerance pathways to desiccation stress in seaweeds, Systems Biology of Marine Ecosystems (2017) 13–33, https://doi.org/10.1007/978-3-319-62094-7_2/FIGURES/2.
[39] L. Contreras-Porcia, D. Thomas, V. Flores, J.A. Correa, Tolerance to oxidative stress induced by desiccation in *Porphyra columbina* (Bangiales, Rhodophyta), J. Exp. Bot. 62 (2011) 1815–1829, https://doi.org/10.1093/JXB/ERQ364.
[40] Y. Ji, J. Tanaka, Effect of desiccation on the photosynthesis of seaweeds from the intertidal zone in Honshu, Japan, Phycological Res. 50 (2002) 145–153, https://doi.org/10.1046/J.1440-1835.2002.00268.X.
[41] M.R. Flores-Molina, D. Thomas, C. Lovazzano, A. Núñez, J. Zapata, M. Kumar, J. A. Correa, L. Contreras-Porcia, Desiccation stress in intertidal seaweeds: effects on morphology, antioxidant responses and photosynthetic performance, Aquat. Bot. 113 (2014) 90–99, https://doi.org/10.1016/J.AQUABOT.2013.11.004.
[42] X. Li, W. Wang, F. Liu, Z. Liang, X. Sun, H. Yao, F. Wang, Periodical drying or no drying during aquaculture affects the desiccation tolerance of a sublittoral *Pyropia yezoensis* strain, J. Appl. Phycol. 30 (2018) 697–705, https://doi.org/10.1007/S10811-017-1227-Y/FIGURES/6.
[43] X. Li, X. Sun, L. Gao, J. Xu, G. Gao, Effects of periodical dehydration on biomass yield and biochemical composition of the edible red alga *Pyropia yezoensis* grown at different salinities, Algal Res. 56 (2021) 102315, https://doi.org/10.1016/J.ALGAL.2021.102315.
[44] J. Templado, E. Ballesteros, I. Galparsoro, Á. Borja, A. Serrano, L. Martín, A. Brito, Inventario español de hábitats y especies marinos. Guía interpretativa: Inventario español de hábitats marinos, 2012.
[45] A. Flores-Moya, D. Moreno, J. De la Rosa, M. Altamirano, E. Bañares-España, Seaweeds and seagrasses: The marine forests from the Alboran Sea, in: Alboran Sea - Ecosystems and Marine Resources, Springer International Publishing, 2021, pp. 247–248, https://doi.org/10.1007/978-3-030-65516-7_8/FIGURES/13.
[46] J. Cai, A. Lovatelli, J. Aguilar-Manjarrez, L. Cornish, L. Dabbadie, A. Desrochers, S. Diffey, E. Garrido Gamarro, J. Geehan, A. Hurtado, D. Lucente, G. Mair, W. Miao, P. Potin, C. Przybyla, M. Reantaso, R. Roubach, M. Tauati, X. Yuan, Seaweeds and Microalgae: An Overview for Unlocking their Potential in Global Aquaculture Development, FAO Fisheries and Aquaculture Circular, Rome, 2021, https://doi.org/10.4060/CB5670EN.
[47] FAO, The State of World Fisheries and Aquaculture 2022. Towards Blue Transformation, FAO, Rome, 2022, https://doi.org/10.4060/CC0461EN.
[48] D. Sahoo, C. Yarish, Chapter 15. Mariculture of seaweeds, in: R.A. Andersen (Ed.), Algal Culturing Technique, Elsevier Academic Press, 2005.
[49] N. Rosic, M. Climstein, G.M. Boyle, D. Thanh Nguyen, Y. Feng, Exploring mycosporine-like amino acid UV-absorbing natural products for a new generation of environmentally friendly sunscreens, Mar. Drugs 21 (2023) 253, https://doi.org/10.3390/MD21040253.
[50] D.G. de Oliveira, G. Schneider, A.G. Itokazu, G.B. Costa, L.R. Rörig, J. C. Simonassi, M. Paes de Barros, F.L. Figueroa, J. Bonomi-Barufi, M. Guimarães, Effects of ultraviolet radiation removal on algal communities in three high-elevation Brazilian (ultra)oligotrophic lakes, Phycologia 60 (2021) 497–512, https://doi.org/10.1080/00318884.2021.1985886.
[51] F.L. Figueroa, J. Aguilera, F.X. Niell, End-of-day light control of growth and pigmentation in the red alga *Porphyra umbilicalis* (L.) Kützing, Zeitschrift Fur Naturforschung - section C, J. Biosci. 49 (1994) 593–600, https://doi.org/10.1515/ZNC-1994-9-1009/MACHINEREADABLECITATION/RIS.
[52] F. López-Figueroa, Red, green and blue light photoreceptors controlling chlorophyll a, biliprotein and total protein synthesis in the red alga *Chondrus crispus*, Br. Phycol. J. 26 (1991) 383–393, https://doi.org/10.1080/00071619100650351.
[53] F. López-Figueroa, F.X. Niell, Red-light and blue-light photoreceptors controlling chlorophyll a synthesis in the red alga *Porphyra umbilicalis* and in the green alga *Ulva rigida*, Physiol. Plant. 76 (1989) 391–397, https://doi.org/10.1111/J.1399-3054.1989.TB06209.X.
[54] F.T. Haxo, L.R. Blinks, Photosynthetic action spectra of marine algae, J. Gen. Physiol. 33 (1950) 389–422, https://doi.org/10.1085/JGP.33.4.389.
[55] L.W. Jones, B. Kok, Photoinhibition of chloroplast reactions. I. Kinetics and action spectra, Plant Physiol. 41 (1966) 1037–1043, https://doi.org/10.1104/PP.41.6.1037.
[56] R.B. Setlow, The wavelengths in sunlight effective in producing skin cancer: a theoretical analysis, Proc. Natl. Acad. Sci. 71 (1974) 3363–3366, https://doi.org/10.1073/PNAS.71.9.3363.
[57] M.M. Caldwell, Solar UV irradiation and the growth and development of higher plants, in: A.C. Giese (Ed.), Photophysiology: Current Topics in Photobiology and Photochemistry, Academic Press, INC., London, 1971.
[58] P. Morliere, A. Moysan, I. Tirache, Action spectrum for UV-induced lipid peroxidation in cultured human skin fibroblasts, Free Radic. Biol. Med. 19 (1995) 365–371, https://doi.org/10.1016/0891-5849(95)00043-W.
[59] L. Provasoli, Media and prospects for cultivation of marine algae, in: A. Watanabe, A. Hattori (Eds.), Cultures and Collections of Algae, Japanese Society of Plant Physiology, 1968, pp. 63–75.
[60] R. Andersen, Algal culturing techniques, Elsevier Academic Press, 2005.
[61] M. Pedersen Lignell, Agar composition as a function of morphology and growth rate. Studies on some morphological strains of *Gracilaria secundata* and *Gracilaria verrucosa* (Rhodophyta), Bot. Mar. 32 (1989) 219–228, https://doi.org/10.1515/BOTM.1989.32.3.219/MACHINEREADABLECITATION/RIS.
[62] K. Grasshoff, K. Kremling, M. Ehrhardt, Methods of Seawater Analysis, 3rd ed., WILEY-VCH, New York, 1999.
[63] G. Johnsen, E. Sakshaug, Biooptical characteristics of PSII and PSI in 33 species (13 pigment groups) of marine phytoplankton, and the relevance for pulse-amplitude-modulated and fast-repetition-rate fluorometry1, J. Phycol. 43 (2007) 1236–1251, https://doi.org/10.1111/J.1529-8817.2007.00422.X.
[64] F.L. Figueroa, R. Conde-Álvarez, I. Gómez, Relations between electron transport rates determined by pulse amplitude modulated chlorophyll fluorescence and oxygen evolution in macroalgae under different light conditions, Photosynth. Res. 75 (2003) 259–275, https://doi.org/10.1023/A:1023936313544/METRICS.
[65] J. Grzymski, G. Johnsen, E. Sakshaug, The significance of intracellular self-shading on the biooptical properties of brown, red, and green macroalgae, J. Phycol. 33 (1997) 408–414, https://doi.org/10.1111/J.0022-3646.1997.00408.X.
[66] P.H.C. Eilers, J.C.H. Peeters, A model for the relationship between light intensity and the rate of photosynthesis in phytoplankton, Ecol. Model. 42 (1988) 199–215, https://doi.org/10.1016/0304-3800(88)90057-9.
[67] S. Beer, A. Eshel, Determining phycoerythrin and phycocyanin concentrations in aqueous crude extracts of red algae, Mar. Freshw. Res. 36 (1985) 785, https://doi.org/10.1071/MF9850785.

[68] R.J. Ritchie, Consistent sets of spectrophotometric chlorophyll equations for acetone, methanol and ethanol solvents, Photosynth. Res. 89 (2006) 27–41, https://doi.org/10.1007/S11120-006-9065-9.

[69] V. Singleton, J. Rossi, Colorimetry of total phenolics with phosphomolybdic-phosphotungstic acid reagents, Am. J. Enol. Vitic. 16 (1965) 144–158.

[70] P. Chaves-Peña, F. De La Coba, F.L. Figueroa, N. Korbee, Quantitative and qualitative HPLC analysis of mycosporine-like amino acids extracted in distilled water for cosmetical uses in four rhodophyta, Mar. Drugs 18 (2020), https://doi.org/10.3390/md18010027.

[71] J. Vega, D. Bárcenas-Pérez, D. Fuentes-Ríos, J.M. López-Romero, P. Hrouzek, F. L. Figueroa, J. Cheel, Isolation of mycosporine-like amino acids from red macroalgae and a marine lichen by high-performance countercurrent chromatography: a strategy to obtain biological UV-filters, Mar. Drugs 21 (2023) 357, https://doi.org/10.3390/MD21060357.

[72] U. Karsten, T. Sawall, D. Hanelt, K. Bischof, F.L. Figueroa, A. Flores-Moya, C. Wiencke, An inventory of UV-absorbing mycosporine-like amino acids in macroalgae from polar to warm-temperate regions, Botanica Marina 41 (1998) 443–453, https://doi.org/10.1515/botm.1998.41.1-6.443.

[73] R. Re, N. Pellegrini, A. Proteggente, A. Pannala, M. Yang, C. Rice-Evans, Antioxidant activity applying an improved ABTS radical cation decolorization assay, Free Radic. Biol. Med. 26 (1999) 1231–1237, https://doi.org/10.1016/S0891-5849(98)00315-3.

[74] W. Brand-Williams, M.E. Cuvelier, C. Berset, Use of a free radical method to evaluate antioxidant activity, LWT Food Sci. Technol. 28 (1995) 25–30, https://doi.org/10.1016/S0023-6438(95)80008-5.

[75] K. Maxwell, G.N. Johnson, Chlorophyll fluorescence—a practical guide, J. Exp. Bot. 51 (2000) 659–668, https://doi.org/10.1093/JEXBOT/51.345.659.

[76] C.G. Jerez, J.R. Malapascua, M. Sergejevová, J. Masojídek, F.L. Figueroa, *Chlorella fusca* (Chlorophyta) grown in thin-layer cascades: estimation of biomass productivity by in-vivo chlorophyll a fluorescence monitoring, Algal Res. 17 (2016) 21–30, https://doi.org/10.1016/J.ALGAL.2016.04.010.

[77] F.L. Figueroa, A. Israel, A. Neori, B. Martínez, E. Jan Malta, P. Ang, S. Inken, R. Marquardt, N. Korbee, Effects of nutrient supply on photosynthesis and pigmentation in *Ulva lactuca* (Chlorophyta): responses to short-term stress, Aquat. Biol. 7 (2009) 173–183, https://doi.org/10.3354/ab00187.

[78] J.B. Barufi, N. Korbee, M.C. Oliveira, F.L. Figueroa, Effects of N supply on the accumulation of photosynthetic pigments and photoprotectors in *Gracilaria tenuistipitata* (Rhodophyta) cultured under UV radiation, J Appl Phycol 23 (2011) 457–466, https://doi.org/10.1007/S10811-010-9603-X/TABLES/3.

[79] J. Bonomi-Barufi, F.L. Figueroa, N. Korbee, M.M. Momoli, A.P. Martins, P. Colepicolo, M.A. Van Sluys, M.C. Oliveira, How macroalgae can deal with radiation variability and photoacclimation capacity: the example of *Gracilaria tenuistipitata* (Rhodophyta) in laboratory, Algal Res. 50 (2020) 102007, https://doi.org/10.1016/j.algal.2020.102007.

[80] K. Lüning, M.J. Dring, Action spectra and spectral quantum yield of photosynthesis in marine macroalgae with thin and thick thalli, Mar. Biol. 87 (1985) 119–129, https://doi.org/10.1007/BF00539419/METRICS.

[81] E.C. Bell, Photosynthetic response to temperature and desiccation of the intertidal alga *Mastocarpus papillatus*, Mar. Biol. 117 (1993) 337–346, https://doi.org/10.1007/BF00345679/METRICS.

[82] D. Zou, K. Gao, Effects of desiccation and CO2 concentrations on emersed photosynthesis in *Porphyra haitanensis* (Bangiales, Rhodophyta), a species farmed in China, Eur. J. Phycol. 37 (2002) 587–592, https://doi.org/10.1017/S0967026202003876.

[83] S. Gao, G. Wang, The enhancement of cyclic electron flow around photosystem I improves the recovery of severely desiccated *Porphyra yezoensis* (Bangiales, Rhodophyta), J. Exp. Bot. 63 (2012) 4349–4358, https://doi.org/10.1093/JXB/ERS082.

[84] B.J. Longstaff, T. Kildea, J.W. Runcie, A. Cheshire, W.C. Dennison, C. Hurd, T. Kana, J.A. Raven, A.W.D. Larkum, An in situ study of photosynthetic oxygen exchange and electron transport rate in the marine macroalga *Ulva lactuca* (Chlorophyta), Photosynth. Res. 74 (2002) 281–293, https://doi.org/10.1023/A:1021279627409.

[85] F. Figueroa, B. Domínguez-González, N. Korbee, Vulnerability and acclimation to increased UVB radiation in three intertidal macroalgae of different morpho-functional groups, Mar. Environ. Res. 97 (2014) 30–38, https://doi.org/10.1016/j.marenvres.2014.01.009.

[86] L. Hendrickson, R.T. Furbank, W.S. Chow, A simple alternative approach to assessing the fate of absorbed light energy using chlorophyll fluorescence, Photosynth. Res. 82 (2004) 73–81, https://doi.org/10.1023/B:PRES.0000040446.87305.F4/METRICS.

[87] É.C. Schmidt, L.A. Scariot, T. Rover, Z.L. Bouzon, Changes in ultrastructure and histochemistry of two red macroalgae strains of <i>Kappaphycus alvarezii< (Rhodophyta, Gigartinales), as a consequence of ultraviolet B radiation exposure, Micron 40 (2009) 860–869, https://doi.org/10.1016/J.MICRON.2009.06.003.

[88] É.C. Schmidt, R. dos Santos, P.A. Horta, M. Maraschin, Z.L. Bouzon, Effects of UVB radiation on the agarophyte *Gracilaria domingensis* (Rhodophyta, Gracilariales): changes in cell organization, growth and photosynthetic performance, Micron 41 (2010) 919–930, https://doi.org/10.1016/J.MICRON.2010.07.010.

[89] F. Álvarez-Gómez, Z.L. Bouzon, N. Korbee, P. Celis-Plá, C. Schmidt, F.L. Figueroa, Combined effects of UVR and nutrients on cell ultrastructure, photosynthesis and biochemistry in *Gracilariopsis longissima* (Gracilariales, Rhodophyta), Algal Res 26 (2017) 190–202, https://doi.org/10.1016/j.algal.2017.07.022.

[90] L. Escassi, J. Aguilera, F.L. Figueroa, J.A. Fernández, Potassium drives daily reversible thallus enlargement in the marine red alga *Porphyra leucosticta* (Rhodophyta), Planta 214 (2002) 759–766, https://doi.org/10.1007/S004250100669/METRICS.

[91] T.J. Cho, M.S. Rhee, Health functionality and quality control of laver (Porphyra, Pyropia): current issues and future perspectives as an edible seaweed, Mar. Drugs 18 (2019) 14, https://doi.org/10.3390/MD18010014.

[92] S.L. Holdt, S. Kraan, Bioactive compounds in seaweed: functional food applications and legislation, J. Appl. Phycol. 23 (2011) 543–597, https://doi.org/10.1007/s10811-010-9632-5.

[93] X. Li, J. Xu, P. He, Comparative research on inorganic carbon acquisition by the macroalgae *Ulva prolifera* (Chlorophyta) and *Pyropia yezoensis* (Rhodophyta), J. Appl. Phycol. 28 (2016) 491–497, https://doi.org/10.1007/S10811-015-0603-8/FIGURES/5.

[94] B.S. Qiu, J.Y. Liu, Utilization of inorganic carbon in the edible cyanobacterium Ge-Xian-Mi (Nostoc) and its role in alleviating photo-inhibition, Plant Cell Environ. 27 (2004) 1447–1458, https://doi.org/10.1111/J.1365-3040.2004.01248.X.

[95] J.K. Kim, G.P. Kraemer, C. Yarish, Emersion induces nitrogen release and alteration of nitrogen metabolism in the intertidal genus porphyra, PloS One 8 (2013) e69961, https://doi.org/10.1371/JOURNAL.PONE.0069961.

[96] T.E. Thomas, D.H. Turpin, P.J. Harrison, Desiccation enhanced nitrogen uptake rates in intertidal seaweeds, Mar. Biol. 94 (1987) 293–298, https://doi.org/10.1007/BF00392943/METRICS.

[97] C.L. Hurd, M.J. Dring, Desiccation and phosphate uptake by intertidal fucoid algae in relation to zonation 26, 1991, pp. 327–333, https://doi.org/10.1080/00071619100650291.

[98] J.K. Kim, G.P. Kraemer, C. Yarish, Physiological activity of Porphyra in relation to eulittoral zonation, J. Exp. Mar. Biol. Ecol. 365 (2008) 75–85, https://doi.org/10.1016/J.JEMBE.2008.07.040.

[99] L.S. Zhao, K. Li, Q.M. Wang, X.Y. Song, H.N. Su, B. Bin Xie, X.Y. Zhang, F. Huang, X.L. Chen, B.C. Zhou, Y.Z. Zhang, Nitrogen Starvation Impacts the Photosynthetic Performance of *Porphyridium cruentum* as Revealed by Chlorophyll a Fluorescence, Scientific Reports (2017) 1–11, https://doi.org/10.1038/s41598-017-08428-6, 2017 7:1 7.

[100] K.K. Sharma, H. Schuhmann, P.M. Schenk, High Lipid Induction in Microalgae for Biodiesel Production, Energies 5 (2012) 1532–1553, https://doi.org/10.3390/EN5051532.

[101] P.P. Lamers, M. Janssen, R.C.H. De Vos, R.J. Bino, R.H. Wijffels, Carotenoid and fatty acid metabolism in nitrogen-starved *Dunaliella salina*, a unicellular green microalga, J. Biotechnol. 162 (2012) 21–27, https://doi.org/10.1016/J.JBIOTEC.2012.04.018.

[102] N. Korbee, P. Huovinen, F.L. Figueroa, J. Aguilera, U. Karsten, Availability of ammonium influences photosynthesis and the accumulation of mycosporine-like amino acids in two Porphyra species (Bangiales, Rhodophyta), Mar. Biol. 146 (2005) 645–654, https://doi.org/10.1007/s00227-004-1484-6.

[103] F. Álvarez-Gómez, N. Korbee, F.L. Figueroa, Effects of UV radiation on photosynthesis, antioxidant capacity and the accumulation of bioactive compounds in *Gracilariopsis longissima*, *Hydropuntia cornea* and *Halopithys incurva* (Rhodophyta), J. Phycol. 55 (2019) 1258–1273, https://doi.org/10.1111/jpy.12899.

[104] U. Karsten, K. Bischof, D. Hanelt, H. Tüg, C. Wiencke, The effect of ultraviolet radiation on photosynthesis and ultraviolet-absorbing substances in the endemic Arctic macroalga *Devaleraea ramentacea* (Rhodophyta), Physiol. Plant. 105 (1999) 58–66, https://doi.org/10.1034/j.1399-3054.1999.105110.x.

[105] H. Jiang, K. Gao, E.W. Helbling, UV-absorbing compounds in *Porphyra haitanensis* (Rhodophyta) with special reference to effects of desiccation, J. Appl. Phycol. 20 (2008) 387–395, https://doi.org/10.1007/S10811-007-9268-2/FIGURES/5.

[106] J.J. Huang, S. Lin, W. Xu, P.C.K. Cheung, Enhancement of the production of bioactive microalgal metabolites by ultraviolet radiation (UVA 365 nm), J. Agric. Food Chem. 66 (2018) 10215–10224, https://doi.org/10.1021/ACS.JAFC.8B03789/ASSET/IMAGES/LARGE/JF-2018-03789C_0004.JPEG.

[107] K. Hoyer, U. Karsten, C. Wiencke, Induction of sunscreen compounds in Antarctic macroalgae by different radiation conditions, Mar. Biol. 141 (2002) 619–627, https://doi.org/10.1007/s00227-002-0871-0.

[108] M.J. Dring, Stress resistance and disease resistance in seaweeds: the role of reactive oxygen metabolism, Adv. Bot. Res. 43 (2005) 175–207, https://doi.org/10.1016/S0065-2296(05)43004-9.